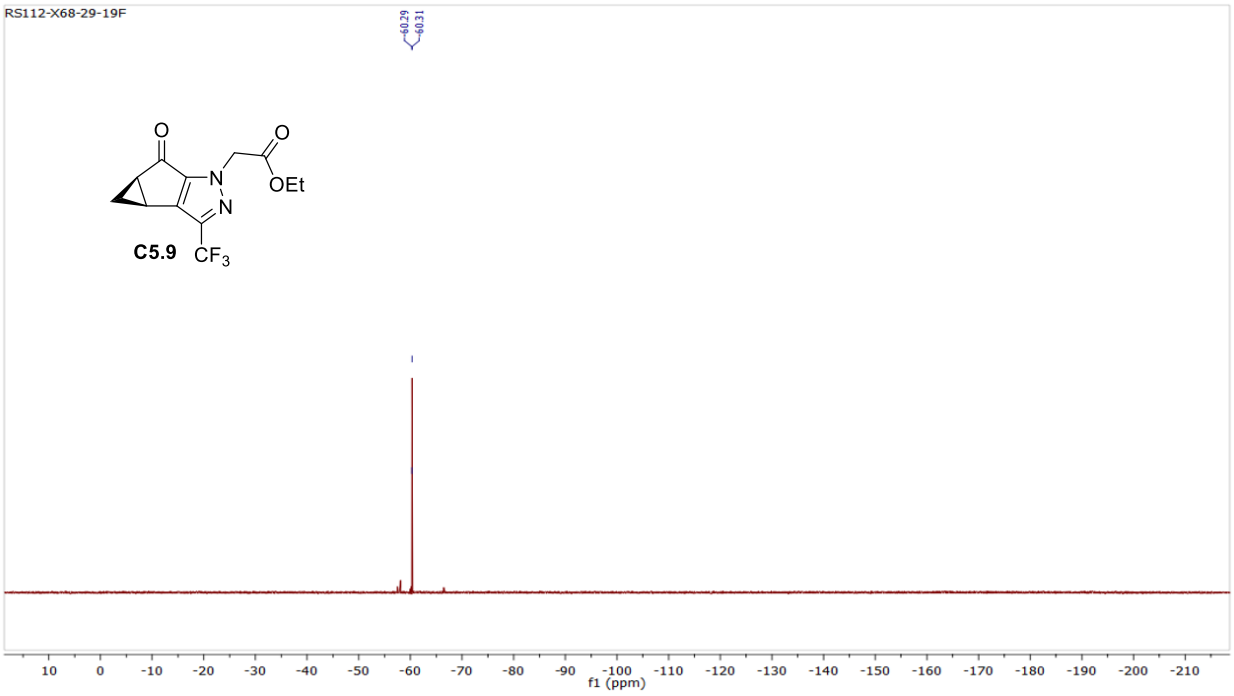

Figure 3.3.23 ^{19}F NMR (565 MHz, DMSO-d_6) of **C5.9**

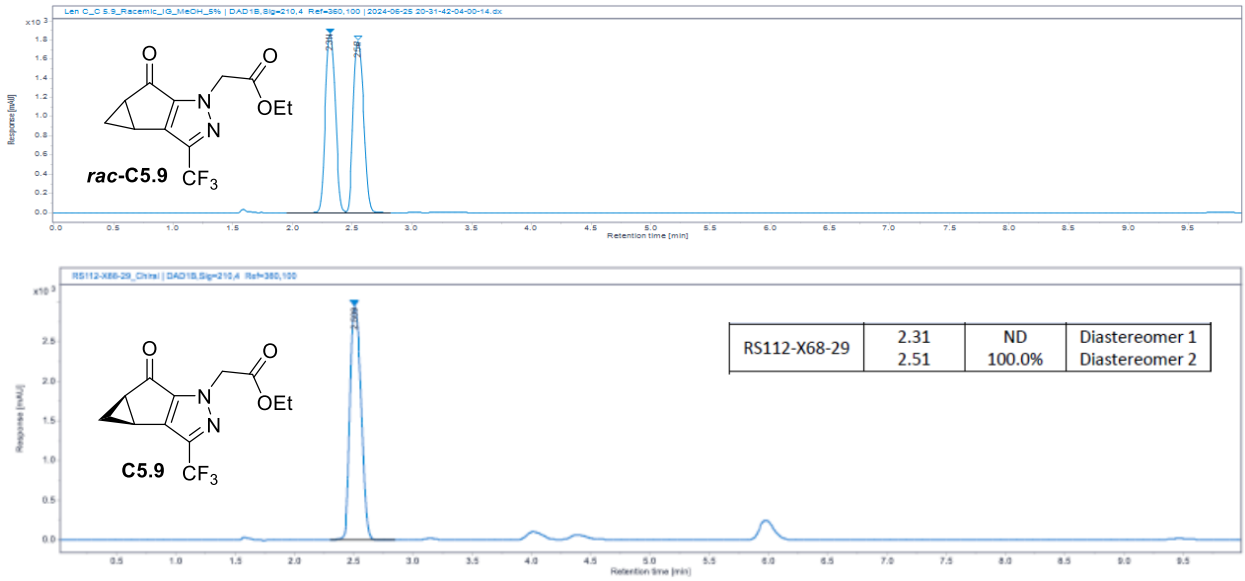

Figure 3.3.24 Chiral GC (GC-FID) spectrum of ***rac*-C5.9** and **C5.9**

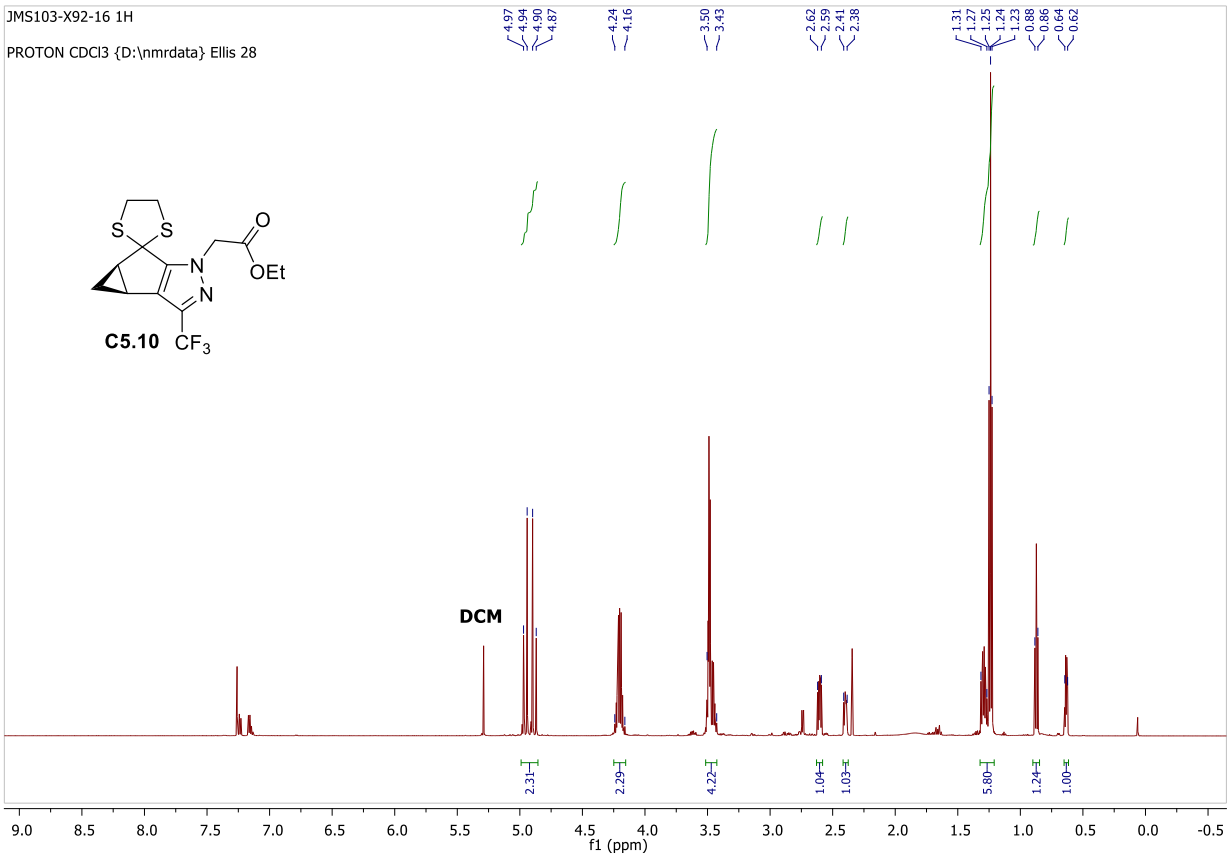

Figure 3.3.25 ^{1}H NMR (600 MHz, $CDCl_3$-*d*) of **C5.10**

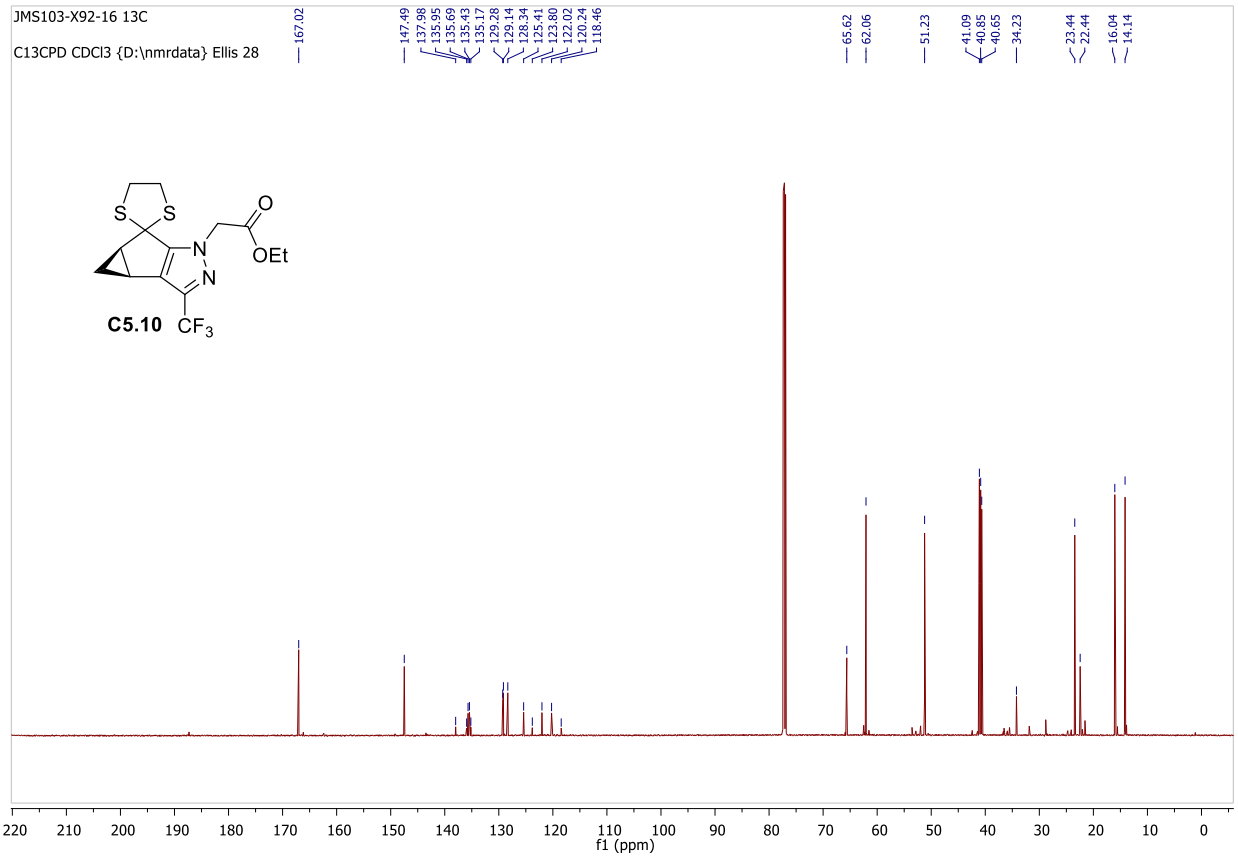

Figure 3.3.26 ^{13}C NMR (150 MHz, $CDCl_3$-*d*) of **C5.10**

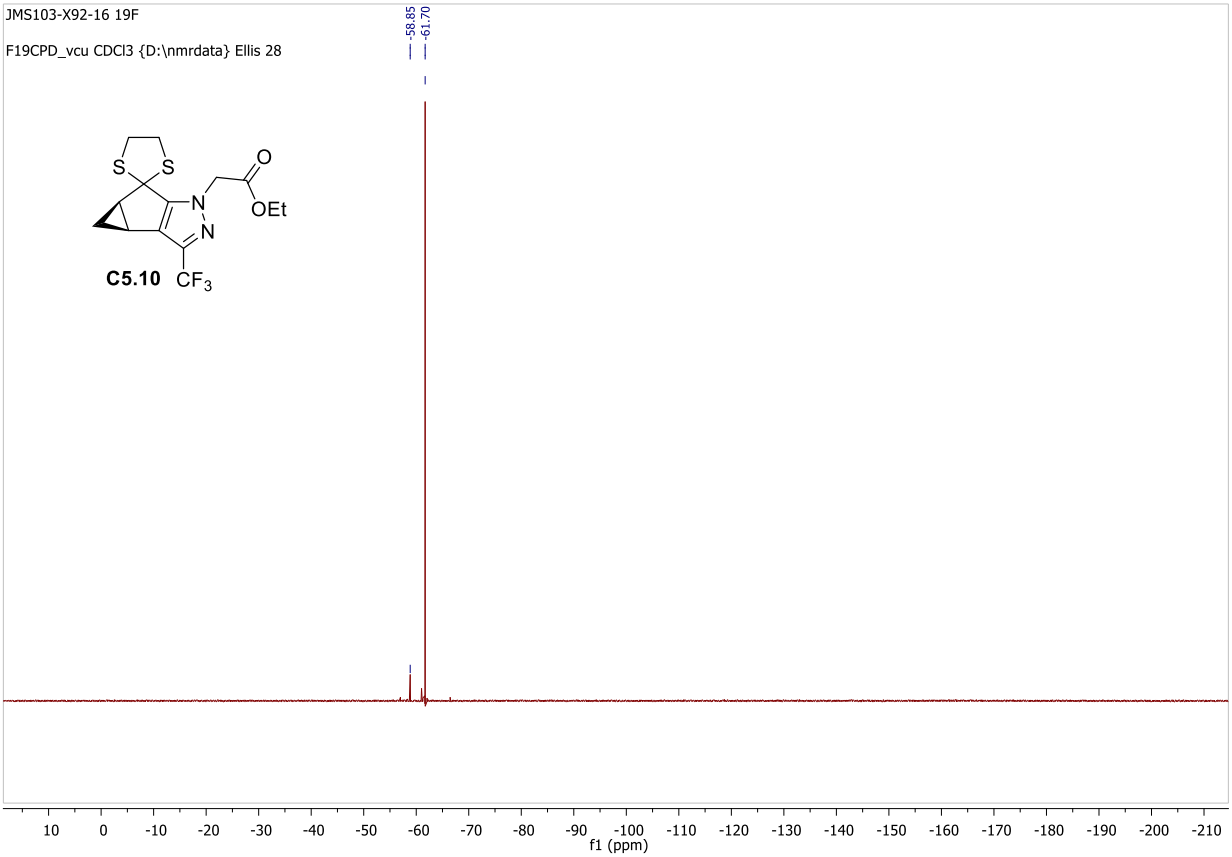

Figure 3.3.27 ^{19}F NMR (565 MHz, $CDCl_3$-*d*) of **C5.10**

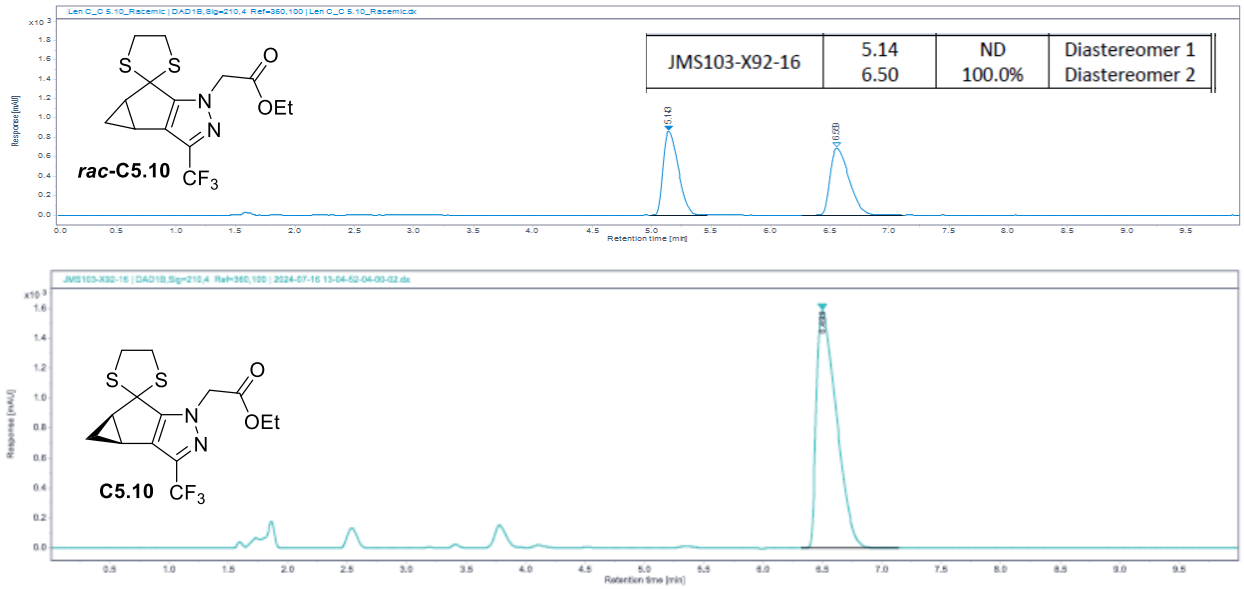

Figure 3.3.28 Chiral GC (GC-FID) spectrum of ***rac*-C5.10** and **C5.10**

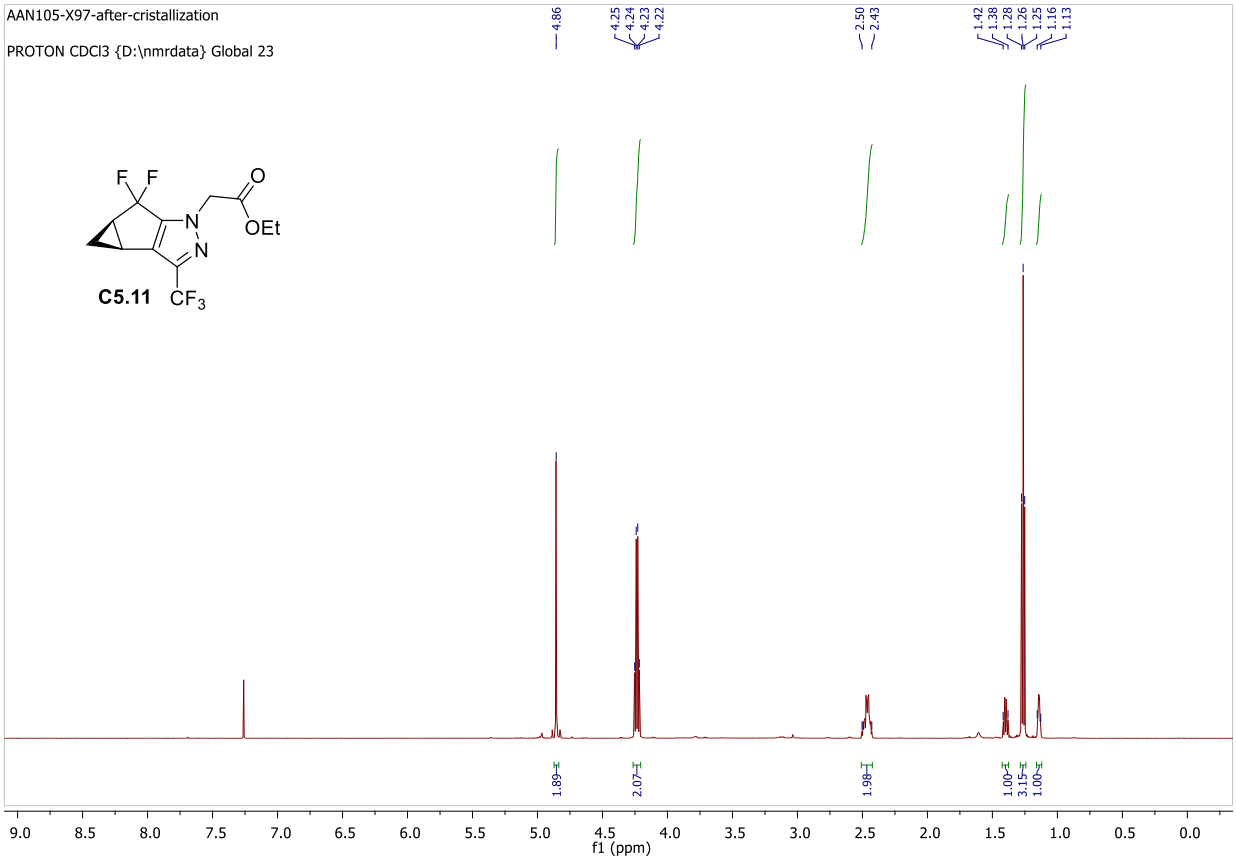

Figure 3.3.29 ^{1}H NMR (600 MHz, $CDCl_3$-*d*) of **C5.11**

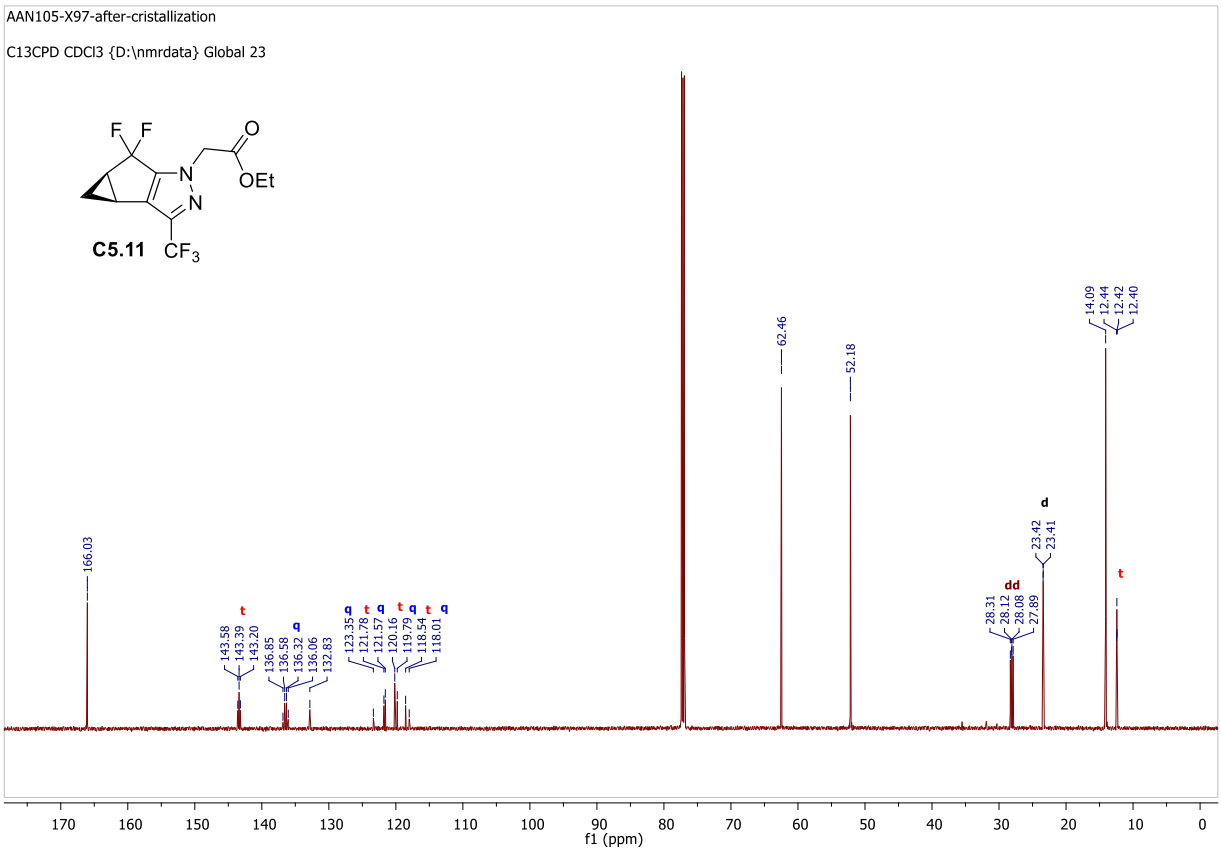

Figure 3.3.30 ^{13}C NMR (150 MHz, $CDCl_3$-*d*) of **C5.11**

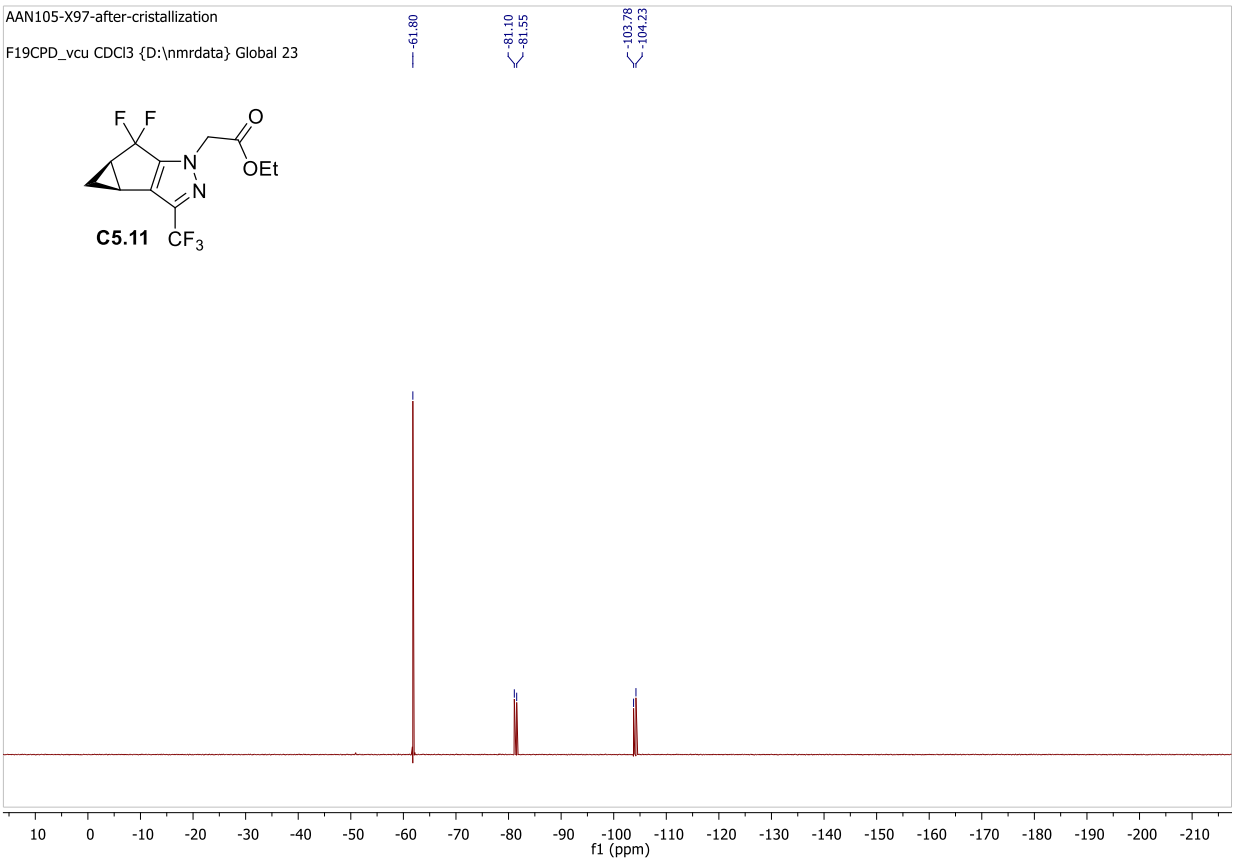

Figure 3.3.31 ^{19}F NMR (564 MHz, $CDCl_3$-*d*) of **C5.11**

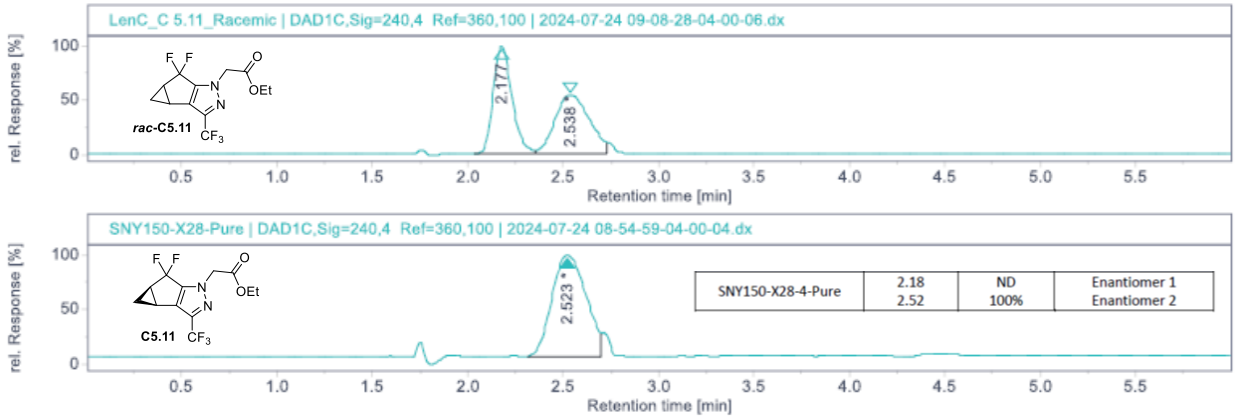

Figure 3.3.32 Chiral GC (GC-FID) spectrum of ***rac*-C5.11** and **C5.11**

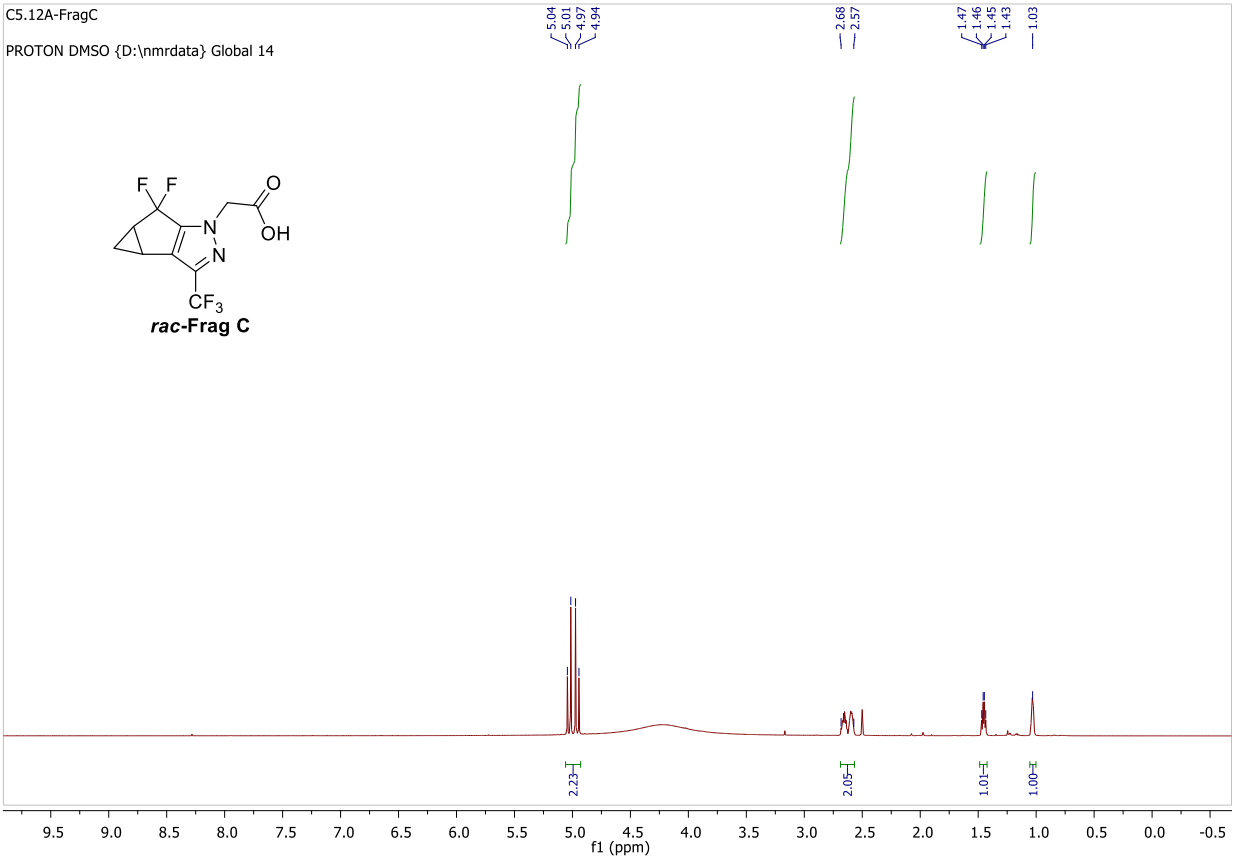

Figure 3.3.33 ^{1}H NMR (600 MHz, DMSO-*d6*) of ***rac*-Frag C**

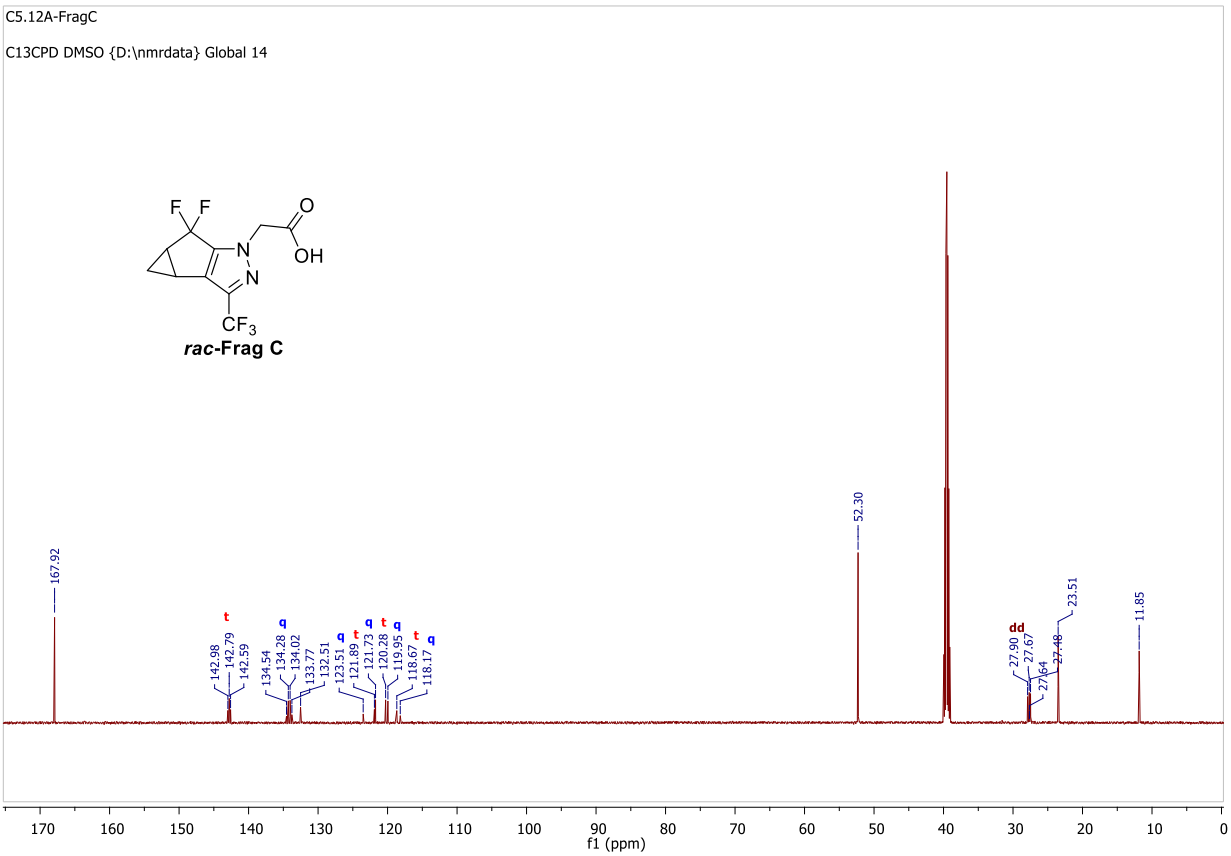

Figure 3.3.34 ^{13}C NMR (600 MHz, DMSO-*d6*) of ***rac*-Frag C**

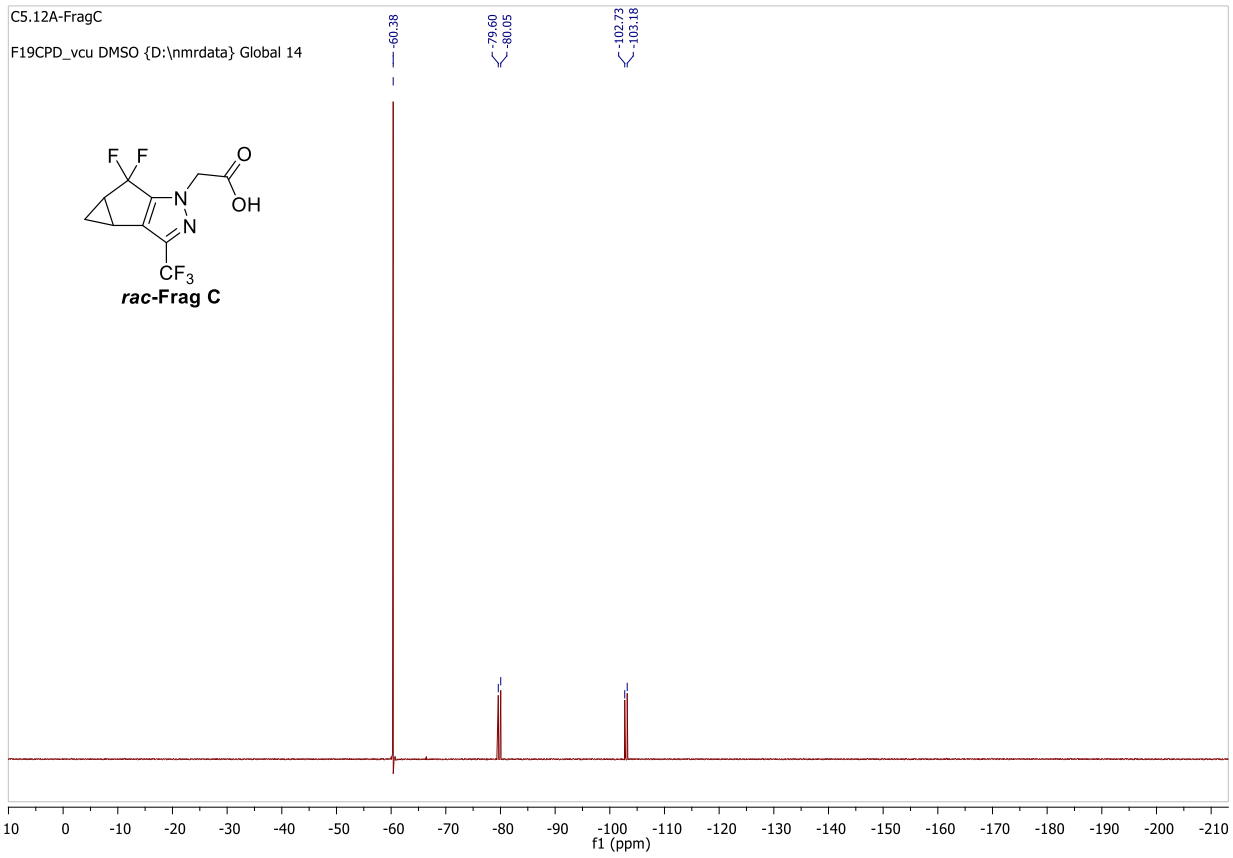

Figure 3.3.35 ^{19}F NMR (600 MHz, DMSO-*d6*) of ***rac*-Frag C**

4 Appendix

4.1 Route scouting of LenC 2

LenC 2 was an asymmetric synthetic approach to access **Frag C**. The key steps include the synthesis of chiral epoxide **C2.6** and the subsequent intramolecular Hodgson cyclopropanation to afford **C2.7** (Scheme 4.1.1).

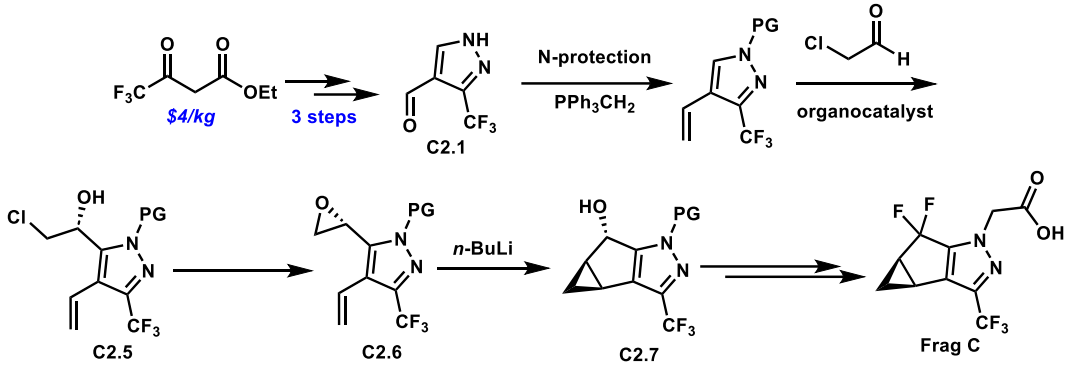

Scheme 4.1.1 Key Idea LenC 2

Unfortunately, the synthesis of precursor **C2.6** turned out to be very challenging. As summarized in Scheme 4.1.2, several routes from the starting material **C2.1** were initially tried, but this substrate proved difficult to functionalize productively. The Boc-protected product (**C2.2**) proved unstable and susceptible to hydrolysis. Tempering the aldehyde's electronic contribution by running the Wittig reaction first, followed by Boc protection, also gave an unstable product. Various bromination conditions with **C2.1** and its acetal-protect analog were explored (Br_2, NBS, HBr/H_2O_2), most showing **C2.1** as unreactive or giving unknown products. *N*-Benzyl protection of **C2.1**, followed by Wittig, is possible, but all attempts failed in the acylation reaction with chloroacetyl chloride under basic conditions (*n*-BuLi, LiTMP, *i*-PrMgCl·LiCl, TMP-MgCl·LiCl), – due to the acidity of the benzylic protons and chloroacetyl chloride reagent. Moreover, *n*-BuLi-promoted polymerization was observed under Hodgson cyclopropanation conditions (i.e., 0 °C), consistent with what is known of the polymerization of styrene by *n*-BuLi.[58]

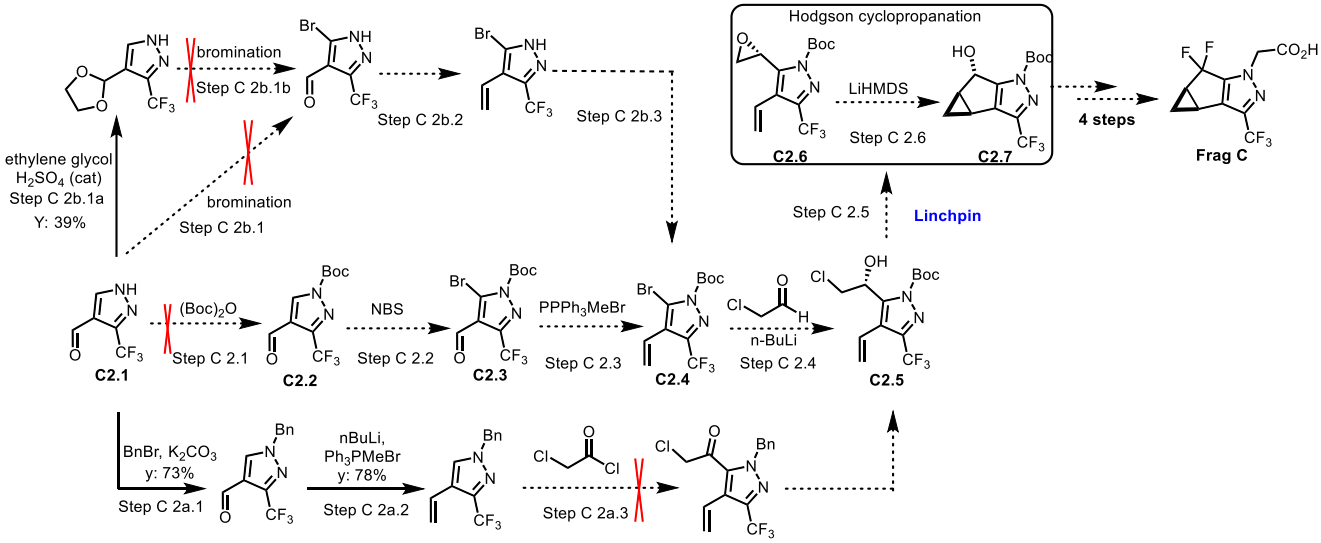

Scheme 4.1.2 Route scouting efforts for Key Idea LenC 2

All the failed results indicated the challenges in the LenC 2 approach. Due to the limited timeline of the project, this approach was abandoned.

4.2 Route scouting of LenC 3

LenC 3 is another asymmetric route to access **Frag C**. The key transformation is desymmetrization of prochiral ketone (**C3.1**) to form chiral trifluoroacetyl bicyclo ketone (**C3.3**) (Scheme 4.2.1). It was envisioned that the desymmetrization could be accomplished via a classic asymmetric aldol reaction organocatalyzed by a chiral secondary amine[59–65] or a Mukaiyama aldol reaction[66–74] from a chiral silyl enol ether. Then the newly formed trifluoroacetyl bicyclo ketone (**C3.3**) could undergo Knorr pyrazole synthesis and be converted to **Frag C** according to the reported method.[5]

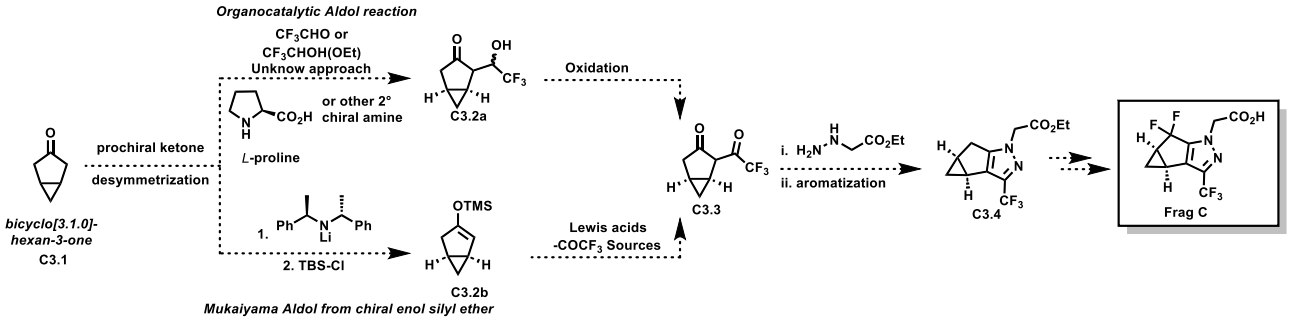

Scheme 4.2.1 Key Idea LenC 3

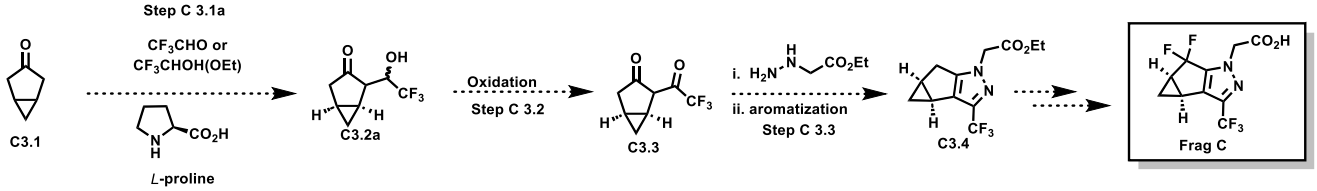

Scheme 4.2.2 Organocatalytic Aldol reaction approach to **Frag C**

Initially, our focus on the organocatalytic Aldol reaction approach to **Frag C** (Scheme 4.2.2). This approach was centered around proline due to its well-known ability to drive asymmetric aldol reactions. Preliminary reactions were done on a model substrate (i.e., cyclohexanone) due to the high cost and low availability of the **C3.1** starting material. The use of this model substrate allowed us to uncover optimal bond-forming conditions for this transformation (i.e., ketone (1.04 eq), (1 eq), DL-proline (30 mol%), MeCN, 25 °C, 24-48 h). Utilizing these conditions, we synthesized ***rac*-C3.2a** in ~80 % assayed yield on a 2-gram scale after 48 h. Regrettably, when chiral amines (Figure 4.2.1) were used in this reaction, only trace amount of product (<10 A% via GCMS) was seen after 4-7 days, and no improvements after heating at 60 ° for 24 h. Isolation and chiral HPLC on **C3.2a** proved unsuccessful due to the complexity and stability of the molecule. Therefore, crude ***rac*-C3.2a** was oxidized under traditional Dess-Martin periodinane (DMP) conditions, affording ***rac*-C3.3** in ~77 % assay yield. Again, isolation and chiral HPLC on ***rac*-C3.3** proved unsuccessful due solely to the complexity of the molecule (i.e., multi-diastereomers and tautomers). Consequently, crude ***rac*-C3.3** was converted to the pyrazole (***rac*-C3.4**) via baseline conditions, affording 160 mg of ***rac*-C3.4** (from 1.01 grams of **C3.1**) in 22 % isolated yield. Nonetheless, these conditions suffer from many drawbacks, including long reaction times, low conversion rates, high amounts of undesired di-substituted byproduct, and expensive and hard-to-obtain bicyclo starting material. Because of this, we abandoned this route.

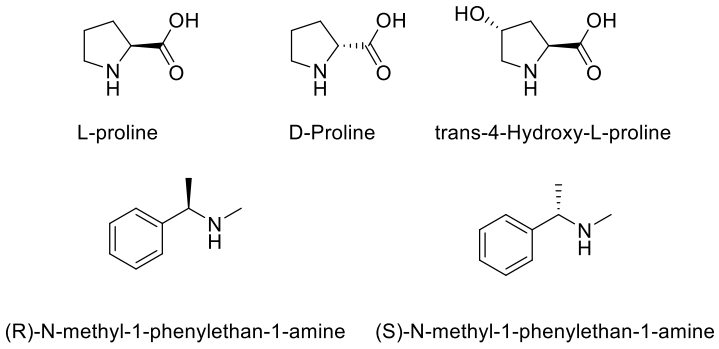

Figure 4.2.1 Chiral secondary amines used in asymmetric aldol condensation

In parallel, we also investigated a modified Mukaiyama aldol reaction (Scheme 4.2.3) to afford **C3.4**. The compound **C3.2b** was prepared in 73 % isolated yield (90 wt% purity by qNMR) from the reaction of **C3.1**, n-BuLi and TBSCl in the presence of (*R*)-*N*-methyl-1-phenylethan-1-amine (Scheme 4.2.2). The measurement of the ee of **C3.2b** was not successful due to the labile of -OTBS functionality. Thus, we moved forward to the next two steps to achieve the pyrazole intermediate **C3.4** to prove the chiral induction concept. In the presence of $Sc(OTf)_3$, the reaction of TFAA with **C3.2b** afforded **C3.3b** in 24% yield and the subsequent Knorr cyclization produced **C3.4** in 41% isolated yield. Regrettably, compound **C3.4** displayed almost racemic (ee <2 %). At the end, this route was abandoned.

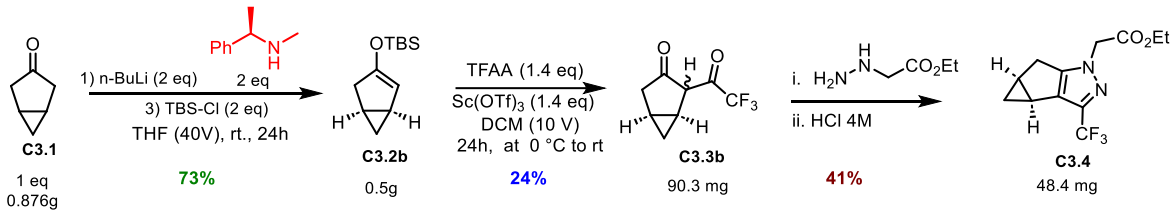

Scheme 4.2.3 Mukaiyama approach to **C3.4**

4.3 Standard operating procedure (SOP) for HF-pyridine chemistry

VCU Safety and Risk Management

medicines for all institute

Standard Operating Procedure

Synthesis of Fluorinated Compounds using Hydrogen Fluoride Pyridine Complex

Print a copy and insert into your
Laboratory Safety Manual and *Chemical Hygiene Plan*.
Refer to instructions for assistance.

Department:	VCU Medicines for All Institutes
Date SOP was written:	June 18, 2024
Date SOP was approved by PI/lab supervisor:	
Principal Investigator:	Frank Gupton 6/20/2024
Internal Lab Safety Coordinator/Lab Manager:	Maria Kubick
Lab Phone:	n/a
Office Phone:	n/a
Emergency Contact:	Maria Kubick 804-337-9919 *(Name and Phone Number)*
Location(s) covered by this SOP:	Biotech 8 Room 301, 302, 303, 304,305 *(Building/Room Number)*

Type of SOP: ☐ Process ☐ Hazardous Chemical

Purpose

The purpose of this document is to detail the steps for setup and usage of a Hydrogen Fluoride Pyridine (HF-Py) complex in laboratories. All users are to read the SOP, SDS, safe work practices, spill control methods, and emergency procedures before starting any work with Hydrofluoric Acid. It is recommended to print a copy of this document and SDS for quick access during any work.
All work shall be performed inside a functioning chemical fume hood, especially during manipulation involving even small quantities of diluted HF solutions. Devices such as single-gas detectors or detection tubes should be deployed in the immediate working area to promote worker awareness with changing conditions. Store the acid deep inside the fume hood and as far away as possible from the user, without obstructing fume hood air flow. Wash your hands thoroughly with soap and water after handling HF.

Click here to enter chemical name or class. 1 Date: Click here to enter a date.

SRM- EH&S Written By/Reviewed By:

VCU Safety and Risk Management

Physical & Chemical Properties/Definition of Chemical Group

CAS#: 62778-11-4

Class: Acute toxicity, Oral (Category 2), H300 Acute toxicity, Inhalation (Category 2), H330 Acute toxicity, Dermal (Category 1), H310 Skin corrosion (Category 1A), H314 Aldrich - 184225 The life science business of Merck KGaA, Darmstadt, Germany operates as MilliporeSigma in the US and Canada Page 1 of 15 Serious eye damage (Category 1), H318 Short-term (acute) aquatic hazard (Category 3), H402

Molecular Formula: C_5H_6FN

Form (physical state): Fuming liquid

Color: clear, colorless

Boiling point: 50°C/ 122°F

Potential Hazards/Toxicity

- Hydrofluoric acid pyridine complex is highly toxic if inhaled. It can cause severe respiratory tract irritation, lung damage, and potentially fatal pulmonary edema.
- It is also highly toxic if ingested. It can cause severe internal burns and systemic toxicity. Do NOT induce vomiting.
- It can cause severe burns that may not be immediately painful but penetrate deeply into tissues, leading to significant damage and systemic toxicity.
- Highly corrosive to most materials, including metals and glass.
- Mixing with water or other reactive substances can result in exothermic reactions, releasing toxic and corrosive fumes.
- It can release fluoride ions, which bind with calcium in the body, causing hypocalcemia and potentially severe cardiac and muscular issues.

Personal Protective Equipment (PPE)

Respirator Protection
n/a

Hand Protection
Neoprene long gloves or Nitrile rubber gloves are ideal for working with hydrofluoric acid pyridine complex, but the thickness may reduce agility. Make sure to test your dexterity before handling this chemical. Always use a Nitrile exam glove underneath to increase your protection.

VCU Safety and Risk Management

Eye Protection
When handling HF, the proper eye protection is ANSI-approved safety goggles and a face shield.

Skin and Body Protection

- **Long sleeves**: Wear a long-sleeved shirt or chemical resistant sleeves.
- **Lab Coat**: Wear a lab coat made of flame-resistant and chemical-resistant material. Ensure the lab coat has a snug fit at the wrists.
- **Apron**: Use a neoprene or PVC apron for additional protection against spills and splashes.
- **Long Pants**: Wear long pants without cuffs to prevent chemicals from lodging near the skin.
- **Closed-Toe Shoes**: Use chemical-resistant footwear, such as rubber or neoprene boots or shoes with non-slip soles.

Figure 1 - Donning of hand, eye, skin, and body PPE

Hygiene Measures
Avoid skin, eye, and clothing contact. Wash hands before breaks and immediately after handling the chemical.

VCU Safety and Risk Management

Engineering Controls

Engineering controls for hydrogen fluoride pyridine (HF-Py) are strategies that reduce the risk of exposure to the chemical by removing it from the air or creating a barrier between the worker and the hazard. Work with this chemical in a certified ducted fume hood. Facilities storing or utilizing this material should be equipped with an eyewash facility and a safety shower

First Aid Procedures

If inhaled

Move inhalation exposure victims to fresh air. Call or have a co-worker call for medical assistance. (Dial 911) Await emergency medical responders, informing them and all others that the exposure involved Hydrogen Fluoride/Hydrofluoric Acid

In case of skin contact

Remove all clothing while in the shower. Immediately flush the affected body area with cold water for a minimum of 5 minutes. Gently apply 2.5% Calcium Gluconate ointment to the affected area while wearing gloves. Call or have a co-worker call for medical assistance. (Dial 911 or (804) 828-9834 for emergency chemical accidents.) Continue to apply the ointment until emergency medical responders arrive.
If calcium gluconate is not immediately available, continue rinsing the affected area with copious amounts of water until emergency medical responders arrive. Inform responders and all others that the exposure involved Hydrogen Fluoride/Hydrofluoric Acid

In case of eye contact

Flush eyes with cold, clean water for at least 15 minutes. Call or have a co-worker call for medical assistance. (Dial 911) Await emergency medical responders, informing them and all others that the exposure involved Hydrogen Fluoride/Hydrofluoric Acid

If swallowed
Call or have a co-worker call for medical assistance (Dial 911 immediately). Drink large amounts of water. Do not induce vomiting. If the injured person is unconscious, turn his/her head or entire body onto the left side. Evacuate the area and move the victim to fresh air.

Special Handling and Storage Requirements

Precautions for safe handling: Avoid contact with skin and eyes. Avoid inhalation and ingestion. Ensure normal measures for preventive fire protection.

Conditions for safe storage: Store in secondary containment with corrosive and acute toxin label on the primary container, secondary containment and the storage location. Keep containers tightly closed in a dry, cool, and well-ventilated place. Protect from moisture. Recommended storage temperature is -20 °C. Avoid strong oxidizing agents, strong bases, strong acids, alkali metals, and metals

Spill and Accident Procedure

Chemical Spill Dial 828-1234 and 828-1392

Spill – Assess the extent of danger. Help contaminated or injured persons. Evacuate the spill area. Avoid breathing vapors. If possible, confine the spill to a small area using a spill kit or absorbent material. Keep others from entering contaminated area (e.g., use caution tape, barriers, etc.).

Small (<1 L) – If you have training, you may assist in the clean-up effort. Use appropriate personal protective equipment and Hydrofluoric acid neutralizing spill kit (**PIG® Hydrofluoric Acid Neutralizing Spill Kit in Bucket**). The bellow spill kit will not contain silica-based materials such as sand or kitty litter. Along with the spill kit, **Sodium Bicarbonate** must be used for spill cleanup. Double bag spill waste in clear plastic bags, label and take to the next chemical waste pick-up.

Large (>1 L) – Dial 828-1234 and EH&S at 828-1392 for assistance.

Chemical Spill on Body or Clothes – Remove clothing and rinse body thoroughly in emergency shower for at least 15 minutes. Seek medical attention. *Notify supervisor and EH&S at 828-1392 immediately.*

Chemical Splash Into Eyes – Immediately rinse eyeball and inner surface of eyelid with water from the emergency eyewash station for 15 minutes by forcibly holding the eye open. Seek medical attention. *Notify supervisor and EH&S at 828-1392 immediately.*

Medical Emergency Dial 828-1234

VCU Safety and Risk Management

Life Threatening Emergency, After Hours, Weekends And Holidays – Dial **828-1234** or contact the VCU Medical Center (emergency room) directly at **(804)828-9000** (located at 1250 Marshall St). *Note: All serious injuries must be reported to EH&S at **828-1392** within 8 hours.*

Non-Life Threatening Emergency – Go to the Employee Health Facility, West Hospital (Room 120) (1200 East Broad Street) Hours: M - W, 8:00 a.m. to 4:00 p.m, T, 8:00 a.m. to 12:30 p.m., F, 8:00 a.m. to 4;00 p.m. At all other times report to VCU Medical Center (emergency room) at **828-9000**. *Note: All serious injuries must be reported to EH&S at 828-1392 within 8 hours.*

Needle stick/puncture exposure (as applicable to chemical handling procedure) – Wash the affected area with antiseptic soap and warm water for 15 minutes. For mucous membrane exposure, flush the affected area for 15 minutes using an eyewash station. Go to the Employee Health Facility, West Hospital (Room 120) (1200 East Broad Street) Hours: M - W, 8:00 a.m. to 4:00 p.m, T, 8:00 a.m. to 12:30 p.m., F, 8:00 a.m. to 4;00 p.m. At all other times report to VCU Medical Center (emergency room) at **828-9000**. *Note: All serious injuries must be reported to EH&S at 828-1392 within 8 hours.*

Decontamination/Waste Disposal Procedure

Liquid: All reaction solutions, products, and waste containing HF-Py will undergo a neutralization step with a saturated aqueous NaHCO3 solution. The solutions will be added to polymer-based waste containers and labeled to denote specific waste stream (organic, aqueous).

Sharps: All needles will be disposed of in labeled non-biohazardous sharps containers.

Solid: All solid waste will be disposed of in labeled, bin-lined, polymer-based, containers

General hazardous waste disposal guidelines:

Label Waste

- Affix a hazardous waste label on all waste containers using the Online label available on VCU's SRM website https://srm.vcu.edu/i-want-to-know-about/waste-management/ as soon as the first drop of waste is added to the container

Store Waste

- Store hazardous waste in closed containers, in secondary containment and in a designated location
- Waste must be under the control of the person generating & disposing of it

Dispose of Waste

- Dispose of regularly generated chemical waste within 90 days
- Call EH&S at 828-1392 for questions or review Hazardous Waster Pick-up Procedure:https://srm.vcu.edu/media/safety-amp-risk-management/assets/Haz%20Chem%20Waste%20Pick%20Up%20Procedures,%20Aug%202017.pdf
- Empty Containers
    - Dispose as hazardous waste if it once held extremely hazardous waste (irrespective of the container size)
    - schedule waste pick-up https://redcap.vcu.edu/surveys/?s=CNF7FWH4LE
        - Check waste label
        - Write date of pick-up request on the waste label
        - Use secondary containment

VCU Safety and Risk Management

Safety Data Sheet (SDS) Location

Online SDS can be accessed at https://www.sigmaaldrich.com/US/en/product/aldrich/184225

Materials and Equipment

- **Lab coat**
- **Safety Goggles**
- **Face Shield**
- **Nitrile gloves**
- **Neoprene Gloves**
- **Polyethylene sleeve**
- **Chemical Resistant shoes**
- **Hydrofluoric Acid Neutralizing Spill Kit in Bucket**
- **Calgonate Calcium GLUCONATE SAFETY KIT**
- **Single Gas Detection Unit (Dräger X-AM 5100 HF/HCl)**

Terminology and References:

- Hydrofluoric Acid (HF) Emergency Exposure Response (https://newpig.scene7.com/is/content/NewPig/pdfs/INST_PLS3900_PLS4000.pdf)
- Calgonate® Emergency First Aid Kit (https://cdn.newpig.com/pds/PLS4000_PDS.pdf)
- CAL OSHA Protecting Workers Exposed to Hydrogen Fluoride (HF) (https://www.dir.ca.gov/dosh/dosh_publications/Hydrogen-Flouride-fs.pdf)

Protocol/Procedure (Add lab specific Protocol/Procedure here)

Read the SOP, SDS, safe work practices, spill control methods, and emergency procedures before starting any work with Hydrofluoric Acid. Also, it is recommended to print a copy of this document and any relevant SDS. Always work inside a functioning chemical fume hood. Keep the acid deep inside the fume hood and as far away as possible from the user.

1. The use of an inert environment is central to any work. A house supply or remote external supply of Nitrogen or other gas should be verified for adequate capacity and viability prior to beginning work.
2. Any reaction vessels shall be composed of polymer-based materials, specifically Polytetrafluoroethylene (PTFE) to contain hazardous chemicals used.

3. Any agitation of solutions may be facilitated through overhead or magnetic stirring. Verify all vessels are adequately sealed and any secondary ports are capped when not in use.
4. Reaction monitoring
    a. Temperature monitoring should be constant through the use of thermocouples with chemically compatible and chemically resistant coatings. A monitoring device such as a J-KEM monitor should be mounted in the primary working area to allow for ease of observation.
    b. Solution pH may be monitored in process using electronic pH meter or sampling solution with pH strips. Verify any meters are functioning and calibrated.
5. Heating or cooling apparatus shall be easily accessible and movable as dictated by a procedure or to manage any hazards or spills.
6. Transfer of reaction materials may be accomplished through the use of a needle with PTFE tubing with a manual plunger, syringe pump, or peristaltic pump. Any device should be secured during use and monitored.
7. Single gas detection devices (e.g. Drager X-AM 5100 detector) should be used in the immediate working area. The minimum acceptable usage is direct attachment of a device to the worker. If extra units are available, they should be placed in close proximity to the reaction vessels and supporting setup.

Work-up: The mixture was quenched with saturated aqueous NaHCO3 (200 mL) solution The suspension was filtered. The mixture was extracted with solvent (50 mL x 3)

Neutralization of HF before sending samples for analysis:

Before submitting the analysis, quench the reaction mixture with saturated aqueous NaHCO3 solution, then extract the mixture with DCM.

4.4 X-ray crystal structure and data

4.4.1 X-ray crystal structure of **C5.9**

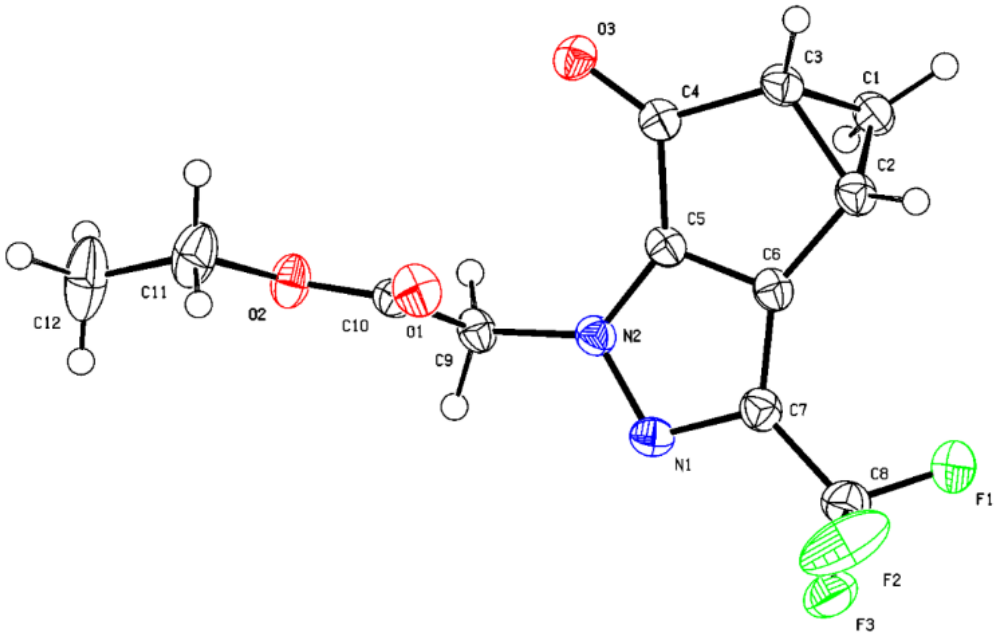

Figure 4.4.1 Single-crystal X-ray structure of **C5.9** with thermal ellipsoids drawn at 50% probability.

4.4.2 X-ray crystal structure data for **C5.9**

Compound	**SNY150-X14a_mC39_offline_auto**
Formula	$C_{12}H_{11}F_3N_2O_3$
$D_{calc.}$/ g cm^{-3}	1.509
μ/mm^{-1}	1.210
Formula Weight	288.23
Colour	clear light colourless
Shape	needle
Size/mm^3	0.75×0.10×0.06
T/K	100.00(10)
Crystal System	monoclinic
Flack Parameter	0.08(8)
Hooft Parameter	0.10(3)
Space Group	$C2$
a/Å	22.0454(3)
b/Å	5.07540(10)
c/Å	11.33730(10)
α/°	90
β/°	90.5160(10)
γ/°	90
V/Å^3	1268.47(3)
Z	4
Z'	1
Wavelength/Å	1.54184
Radiation type	Cu K_α
Θ_{min}/°	3.899
Θ_{max}/°	74.955
Measured Refl.	21071
Independent Refl.	2422
Reflections with I > 2(I)	2417
R_{int}	0.0433
Parameters	183
Restraints	1
Largest Peak	0.408
Deepest Hole	-0.337
GooF	1.052
wR_2 (all data)	0.0851
wR_2	0.0850
R_1 (all data)	0.0331
R_1	0.0330

Table 4.4.1: Fractional Atomic Coordinates (×10⁴) and Equivalent Isotropic Displacement Parameters (Å²×10³) for **SNY150-X14a_mC39_offline_auto**. U_{eq} is defined as 1/3 of the trace of the orthogonalised U_{ij}.

Atom	x	y	z	U_{eq}
F3	5132.8(7)	715(4)	2534.5(15)	38.5(4)
O3	7531.0(7)	8670(3)	4179.6(14)	25.3(4)
O2	8232.5(7)	4414(4)	1325.3(14)	28.9(4)
O1	7430.4(8)	7156(4)	1124.7(16)	31.3(4)
F1	4854.3(7)	3617(5)	3762.0(19)	62.0(7)
F2	4928.0(9)	4579(5)	1919(2)	67.6(7)
N2	6791.0(9)	4106(4)	2765.9(16)	22.6(4)
N1	6278.1(9)	2896(4)	2412.4(17)	24.8(5)
C5	6668.5(10)	6043(5)	3550.4(19)	21.5(5)
C4	6997.9(10)	8057(5)	4236.9(19)	21.7(5)
C6	6056.2(10)	6092(5)	3743(2)	22.8(5)
C10	7668.4(11)	5227(5)	1525(2)	23.5(5)
C9	7378.1(10)	3248(5)	2349(2)	23.3(5)
C8	5192.0(12)	3275(6)	2797(2)	32.1(6)
C2	5906.3(11)	8054(5)	4674(2)	24.9(5)
C1	6192.3(11)	7477(5)	5855(2)	26.8(6)
C7	5828.1(10)	4077(6)	3013(2)	25.2(5)
C3	6516.0(11)	9296(5)	4992(2)	25.0(5)
C11	8592.1(13)	5945(8)	497(2)	41.3(8)
C12	9102.5(14)	4236(10)	111(3)	56.8(11)

Table 4.4.2: Anisotropic Displacement Parameters (×10⁴) **SNY150-X14a_mC39_offline_auto**. The anisotropic displacement factor exponent takes the form: $-2\pi^2[h^2a^{*2} \times U_{11} + \ldots + 2hka^* \times b^* \times U_{12}]$

Atom	U_{11}	U_{22}	U_{33}	U_{23}	U_{13}	U_{12}
F3	31.1(8)	35.5(11)	49.0(9)	-4.0(8)	-2.7(7)	-8.0(7)
O3	25.7(8)	18.5(10)	31.8(8)	3.2(7)	2.6(6)	-2.7(7)
O2	24.8(8)	34.9(12)	27.1(8)	10.0(8)	4.8(6)	1.5(8)
O1	38.3(10)	23.4(10)	32.3(9)	5.3(8)	3.8(7)	4.5(8)
F1	29.1(8)	88.9(18)	68.1(12)	-41.0(12)	12.6(8)	-7.8(10)
F2	52.5(11)	53.6(14)	95.7(16)	32.8(12)	-44.4(11)	-13.8(10)
N2	24.8(9)	20.2(11)	22.9(9)	-1.2(8)	1.7(7)	-0.1(8)
N1	27.3(9)	21.2(12)	25.9(9)	-2.5(8)	-1.0(7)	-1.0(8)
C5	27.2(11)	15.3(12)	21.9(10)	1.4(9)	2.6(8)	0.5(9)
C4	27.7(11)	13.5(12)	24.0(10)	3.8(9)	2.3(8)	0.3(9)
C6	25.0(11)	19.8(13)	23.5(10)	1.0(9)	2.5(8)	2.4(9)
C10	26.8(11)	23.2(15)	20.3(10)	-2.1(9)	0.5(8)	-1.5(10)
C9	26.2(10)	19.4(13)	24.4(10)	-0.2(9)	4.1(8)	4.3(10)
C8	30.8(12)	30.3(17)	35.2(13)	-5.8(11)	-2.9(10)	1.6(11)
C2	26.4(11)	20.0(13)	28.2(11)	-1.2(10)	3.2(9)	2.9(10)
C1	30.5(12)	25.8(16)	24.2(11)	-3.0(9)	4.5(9)	-0.3(10)
C7	24.8(11)	24.9(14)	26.0(10)	-1.0(11)	0.1(8)	3.4(10)
C3	28.4(11)	17.2(14)	29.4(11)	-3.2(10)	2.7(9)	1.7(10)

Atom	U_{11}	U_{22}	U_{33}	U_{23}	U_{13}	U_{12}
C11	33.0(13)	55(2)	35.7(14)	18.6(14)	7.5(11)	-2.9(14)
C12	34.3(15)	92(3)	44.8(16)	30(2)	14.4(12)	14.4(18)

Table 4.4.3: Bond Lengths in Å for **SNY150-X14a_mC39_offline_auto**.

Atom	Atom	Length/Å
F3	C8	1.339(4)
O3	C4	1.218(3)
O2	C10	1.331(3)
O2	C11	1.458(3)
O1	C10	1.198(3)
F1	C8	1.340(3)
F2	C8	1.326(3)
N2	N1	1.345(3)
N2	C5	1.355(3)
N2	C9	1.449(3)
N1	C7	1.349(3)
C5	C4	1.472(3)
C5	C6	1.370(3)
C4	C3	1.508(3)
C6	C2	1.490(3)
C6	C7	1.406(4)
C10	C9	1.517(3)
C8	C7	1.478(3)
C2	C1	1.504(3)
C2	C3	1.525(3)
C1	C3	1.527(3)
C11	C12	1.489(5)

Table 4.4.42: Bond Angles in ° for **SNY150-X14a_mC39_offline_auto**.

Atom	Atom	Atom	Angle/°
C10	O2	C11	117.3(2)
N1	N2	C5	110.79(19)
N1	N2	C9	121.1(2)
C5	N2	C9	128.0(2)
N2	N1	C7	105.49(19)
N2	C5	C4	138.7(2)
N2	C5	C6	108.7(2)
C6	C5	C4	112.6(2)
O3	C4	C5	128.4(2)
O3	C4	C3	127.5(2)
C5	C4	C3	104.08(19)
C5	C6	C2	110.5(2)

Atom	Atom	Atom	Angle/˚
C5	C6	C7	103.9(2)
C7	C6	C2	145.4(2)
O2	C10	C9	107.4(2)
O1	C10	O2	126.5(2)
O1	C10	C9	126.0(2)
N2	C9	C10	112.7(2)
F3	C8	F1	104.7(2)
F3	C8	C7	113.2(2)
F1	C8	C7	111.3(2)
F2	C8	F3	106.0(2)
F2	C8	F1	107.8(3)
F2	C8	C7	113.3(3)
C6	C2	C1	114.0(2)
C6	C2	C3	104.08(19)
C1	C2	C3	60.55(16)
C2	C1	C3	60.40(16)
N1	C7	C6	111.1(2)
N1	C7	C8	119.7(2)
C6	C7	C8	129.1(2)
C4	C3	C2	108.5(2)
C4	C3	C1	116.6(2)
C2	C3	C1	59.05(16)
O2	C11	C12	107.2(3)

Table 4.4.5: Torsion Angles in ˚ for **SNY150-X14a_mC39_offline_auto**.

Atom	Atom	Atom	Atom	Angle/˚
F3	C8	C7	N1	33.2(3)
F3	C8	C7	C6	-150.7(3)
O3	C4	C3	C2	174.3(2)
O3	C4	C3	C1	-121.7(3)
O2	C10	C9	N2	171.85(19)
O1	C10	C9	N2	-8.5(3)
F1	C8	C7	N1	150.8(3)
F1	C8	C7	C6	-33.1(4)
F2	C8	C7	N1	-87.6(3)
F2	C8	C7	C6	88.5(3)
N2	N1	C7	C6	1.0(3)
N2	N1	C7	C8	177.7(2)
N2	C5	C4	O3	7.4(5)
N2	C5	C4	C3	-175.4(3)
N2	C5	C6	C2	175.48(19)
N2	C5	C6	C7	-0.5(3)
N1	N2	C5	C4	-178.8(3)
N1	N2	C5	C6	1.2(3)

Atom	Atom	Atom	Atom	Angle/˚
N1	N2	C9	C10	110.6(3)
C5	N2	N1	C7	-1.3(3)
C5	N2	C9	C10	-71.9(3)
C5	C4	C3	C2	-3.0(3)
C5	C4	C3	C1	61.0(3)
C5	C6	C2	C1	-61.4(3)
C5	C6	C2	C3	2.3(3)
C5	C6	C7	N1	-0.3(3)
C5	C6	C7	C8	-176.7(3)
C4	C5	C6	C2	-4.5(3)
C4	C5	C6	C7	179.5(2)
C6	C5	C4	O3	-172.6(2)
C6	C5	C4	C3	4.6(3)
C6	C2	C1	C3	93.1(2)
C6	C2	C3	C4	0.6(3)
C6	C2	C3	C1	-109.9(2)
C10	O2	C11	C12	-161.2(3)
C9	N2	N1	C7	176.6(2)
C9	N2	C5	C4	3.5(5)
C9	N2	C5	C6	-176.5(2)
C2	C6	C7	N1	-173.7(3)
C2	C6	C7	C8	9.9(6)
C2	C1	C3	C4	-96.5(2)
C1	C2	C3	C4	110.5(2)
C7	C6	C2	C1	111.8(4)
C7	C6	C2	C3	175.5(3)
C11	O2	C10	O1	-3.0(4)
C11	O2	C10	C9	176.7(2)

Table 4.4.6: Hydrogen Fractional Atomic Coordinates (×10⁴) and Equivalent Isotropic Displacement Parameters (Å²×10³) for **SNY150-X14a_mC39_offline_auto**. U_{eq} is defined as 1/3 of the trace of the orthogonalised U_{ij}.

Atom	x	y	z	U_{eq}
H9A	7330.39	1546.41	1931.68	28
H9B	7650.81	2956.11	3035.17	28
H2	5531.43	9156.5	4611.4	30
H1A	6364.24	5696.92	5983.45	32
H1B	6006.93	8285.94	6560.23	32
H3	6536.15	11227.06	5163.22	30
H11A	8750.59	7555.99	884.06	50
H11B	8340.15	6473.64	-190.03	50
H12A	9374.66	5252.03	-393.8	85
H12B	8941.08	2728	-330.68	85
H12C	9327.45	3603.23	805.06	85

4.4.3 X-ray crystal structure of **C5.11**

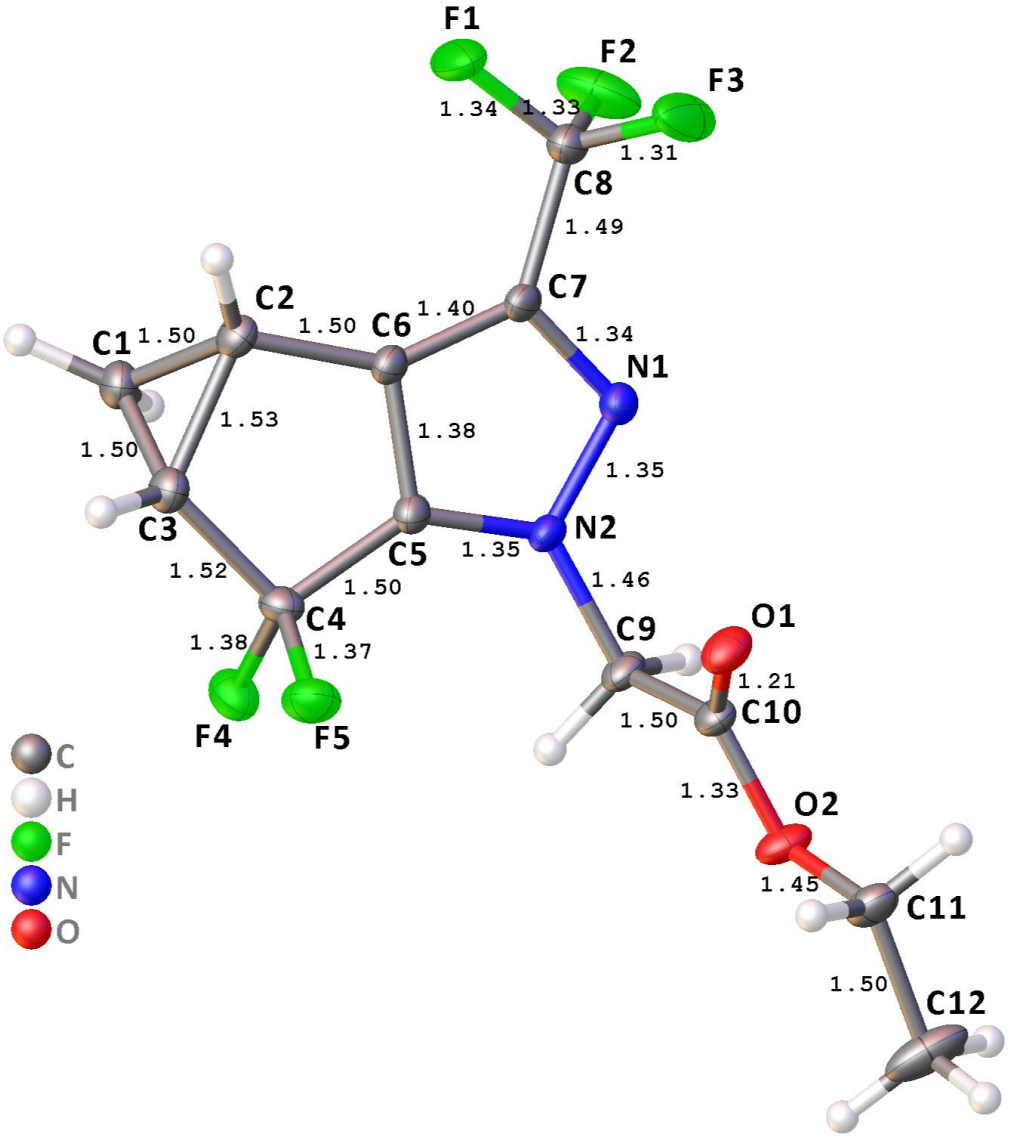

Figure 4.4.2 Single-crystal X-ray structure of **C5.11** with thermal ellipsoids drawn at 50% probability.

4.4.4 X-ray crystal structure data for **C5.11**

Table 4.4.7 Fractional Atomic Coordinates ($\times 10^4$) and Equivalent Isotropic Displacement Parameters ($Å^2 \times 10^3$) for **C5.11**. U_{eq} is defined as 1/3 of the trace of the orthogonalised U_{ij}.

Atom	x	y	z	U_{eq}
F10	873(4)	3845(3)	6650(3)	38.4(7)
F9	-858(4)	2861(3)	5437(3)	41.8(7)
F5	6508(4)	6310(3)	3382(3)	44.5(7)
F4	4379(4)	7397(3)	4472(3)	41.5(7)
O4	3642(4)	-727(3)	7914(3)	32.8(7)
F1	8695(5)	5621(3)	9441(3)	61.5(11)
O3	4661(5)	1493(3)	6806(3)	39.0(8)
O1	10356(5)	8683(3)	3358(4)	37.8(8)
O2	9433(5)	10798(3)	2171(3)	35.9(8)
F2	8661(6)	7929(4)	9774(4)	69.1(11)
F3	10741(5)	7036(6)	8556(4)	77.7(13)
N4	2750(5)	1449(4)	4591(4)	28.3(8)
N2	7682(5)	8623(4)	5505(4)	27.6(8)
N3	4028(5)	1370(4)	3535(4)	31.7(8)
N1	8575(5)	8656(4)	6628(4)	30.5(8)
C10	9341(6)	9678(4)	3257(4)	29.2(9)
C8	9113(6)	6990(5)	8788(5)	32.8(10)
C17	2023(6)	2816(4)	4493(4)	26.2(8)
C19	4057(6)	2718(5)	2722(4)	29.9(9)
C6	7232(5)	6428(4)	6840(4)	25.8(8)
C18	2805(6)	3667(4)	3284(4)	26.4(8)
C7	8294(6)	7327(4)	7434(4)	27.0(9)
C5	6895(6)	7304(4)	5587(4)	26.4(9)
C2	6296(6)	4984(4)	7032(4)	28.9(9)
C4	5771(6)	6544(5)	4740(4)	29.2(9)
C22	3758(6)	437(4)	6867(4)	26.8(9)
C16	626(6)	3636(4)	5252(4)	28.3(9)
C21	2521(6)	248(4)	5804(5)	29.9(9)
C14	1989(6)	5163(4)	3056(4)	30.7(9)
C9	7804(6)	9844(4)	4314(5)	31.3(10)
C15	573(6)	5123(5)	4301(5)	31.1(9)
C3	5361(6)	5073(5)	5694(5)	32.3(10)
C1	4442(6)	5178(5)	7176(5)	36.0(10)
C13	198(7)	5084(5)	2775(5)	36.9(11)
C23	4695(7)	-630(5)	9066(5)	36.8(11)
C11	10823(7)	10749(5)	1031(5)	37.5(11)
C20	5353(7)	3062(6)	1449(5)	40.7(11)
C24	4376(8)	-2030(6)	10150(5)	47.1(13)
C12	10604(10)	12011(7)	-137(6)	65(2)
F8	4856(8)	3872(12)	445(7)	225(6)
F6	6715(6)	3597(6)	1822(5)	93.4(17)
F7	5988(7)	1817(6)	932(5)	103(2)

Table 4.4.8 Anisotropic Displacement Parameters ($\times 10^4$) **C5.11**. The anisotropic displacement factor exponent takes the form: $-2p^2[h^2a^{*2} \times U_{11} + ... + 2hka^* \times b^* \times U_{12}]$

Atom	U_{11}	U_{22}	U_{33}	U_{23}	U_{13}	U_{12}
F10	44.4(18)	42.4(14)	25.8(11)	5.4(10)	-3.6(11)	-0.2(12)
F9	30.9(17)	36.5(14)	55.6(16)	1.1(11)	-1.7(13)	-5.5(12)
F5	55(2)	48.3(15)	30.6(12)	-2.1(10)	-10.6(13)	-0.4(14)
F4	38.4(18)	36.6(13)	51.9(16)	-2.2(11)	-17.7(14)	1.0(12)
O4	39(2)	27.9(14)	30.1(14)	8.0(11)	-9.0(13)	-4.5(13)
F1	87(3)	48.2(16)	49.5(17)	23.0(13)	-34.6(18)	-26.0(17)
O3	46(2)	34.0(15)	36.3(16)	6.6(12)	-9.1(15)	-15.1(14)
O1	35(2)	31.0(15)	42.6(17)	11.1(12)	-2.7(14)	3.1(13)
O2	44(2)	30.6(14)	28.2(14)	10.4(11)	0.4(13)	6.3(13)
F2	91(3)	77(2)	49.8(18)	-21.9(16)	-40(2)	23(2)
F3	32(2)	143(4)	51.5(19)	30(2)	-16.1(16)	-17(2)
N4	25(2)	26.2(15)	31.0(17)	5.5(13)	-3.0(14)	-1.1(14)
N2	25(2)	28.8(16)	26.6(16)	7.9(13)	-4.3(14)	-5.7(14)
N3	28(2)	36.4(18)	29.7(17)	2.9(14)	-5.6(15)	-1.9(16)
N1	26(2)	33.0(17)	31.7(17)	4.0(13)	-6.4(15)	-6.7(15)
C10	34(3)	24.2(18)	28.2(19)	6.3(14)	-7.9(17)	-5.0(17)
C8	29(3)	40(2)	29(2)	4.8(16)	-7.4(18)	-7.0(18)
C17	23(2)	25.2(18)	28.1(18)	6.6(14)	-4.7(15)	-4.5(15)
C19	30(3)	35(2)	23.9(18)	2.1(15)	-8.4(17)	-5.2(17)
C6	21(2)	28.4(18)	25.9(18)	3.7(14)	-1.8(16)	-3.9(16)
C18	23(2)	31.6(19)	23.1(17)	6.2(14)	-5.4(15)	-4.3(16)
C7	21(2)	33.0(19)	24.6(18)	5.3(15)	-1.3(16)	-5.3(17)
C5	22(2)	27.2(18)	29.1(18)	3.1(14)	-4.7(16)	-3.5(16)
C2	33(3)	22.2(17)	30.4(19)	1.9(14)	-3.4(18)	-3.3(17)
C4	32(3)	29.8(19)	26.9(18)	0.1(15)	-10.7(17)	0.8(17)
C22	26(3)	24.3(18)	27.2(18)	4.2(14)	-0.3(16)	-0.4(16)
C16	28(3)	29.0(19)	25.5(18)	6.2(14)	-2.5(16)	-5.3(16)
C21	28(3)	24.2(18)	36(2)	9.7(15)	-7.9(18)	-3.3(17)
C14	37(3)	27.2(19)	25.3(18)	6.4(15)	-4.4(17)	-4.2(17)
C9	32(3)	26.1(19)	32(2)	11.2(15)	-3.7(18)	-2.4(17)
C15	32(3)	27.9(19)	31(2)	6.3(16)	-1.3(18)	0.6(17)
C3	35(3)	27.4(19)	35(2)	-0.5(16)	-6.5(19)	-6.8(18)
C1	34(3)	34(2)	39(2)	1.9(17)	-8(2)	-11.5(19)
C13	40(3)	37(2)	32(2)	4.3(17)	-9(2)	6(2)
C23	37(3)	45(2)	27(2)	6.5(17)	-6.3(19)	-2(2)
C11	48(3)	36(2)	25.6(19)	3.8(16)	0.5(19)	-3(2)
C20	43(3)	51(3)	26(2)	-0.9(18)	-1(2)	-5(2)
C24	59(4)	48(3)	31(2)	11(2)	-10(2)	0(2)
C12	89(6)	52(3)	40(3)	18(2)	23(3)	20(3)

Atom	U_{11}	U_{22}	U_{33}	U_{23}	U_{13}	U_{12}
F8	91(4)	409(13)	102(4)	176(6)	64(3)	125(6)
F6	74(3)	129(4)	76(3)	-43(3)	35(2)	-62(3)
F7	106(4)	107(3)	92(3)	-54(3)	57(3)	-47(3)

Table 4.4.9 Bond Lengths in Å for **C5.11**.

Atom	Atom	Length/ Å	Atom	Atom	Length/ Å
F10	C16	1.374(5)	C17	C18	1.372(5)
F9	C16	1.380(5)	C17	C16	1.487(7)
F5	C4	1.366(5)	C19	C18	1.402(7)
F4	C4	1.381(5)	C19	C20	1.487(7)
O4	C22	1.337(5)	C6	C7	1.395(6)
O4	C23	1.460(5)	C6	C5	1.379(5)
F1	C8	1.335(5)	C6	C2	1.495(5)
O3	C22	1.199(5)	C18	C14	1.490(6)
O1	C10	1.205(6)	C5	C4	1.497(6)
O2	C10	1.334(5)	C2	C3	1.527(6)
O2	C11	1.451(6)	C2	C1	1.497(7)
F2	C8	1.332(6)	C4	C3	1.519(5)
F3	C8	1.308(6)	C22	C21	1.516(6)
N4	N3	1.342(5)	C16	C15	1.515(5)
N4	C17	1.350(5)	C14	C15	1.522(6)
N4	C21	1.461(5)	C14	C13	1.507(7)
N2	N1	1.345(5)	C15	C13	1.492(6)
N2	C5	1.345(5)	C3	C1	1.495(7)
N2	C9	1.459(5)	C23	C24	1.519(6)
N3	C19	1.348(5)	C11	C12	1.498(6)
N1	C7	1.339(5)	C20	F8	1.218(6)
C10	C9	1.502(7)	C20	F6	1.311(7)
C8	C7	1.491(5)	C20	F7	1.338(7)

Table 4.4.10 Bond Angles in ° for **C5.11**.

Atom	Atom	Atom	Angle/°	Atom	Atom	Atom	Angle/°
C22	O4	C23	114.9(3)	C6	C2	C1	113.8(4)
C10	O2	C11	116.3(4)	C1	C2	C3	59.2(3)
N3	N4	C17	111.5(3)	F5	C4	F4	104.0(3)

N3	N4	C21	119.3(4)	F5	C4	C5	113.0(4)
C17	N4	C21	128.0(4)	F5	C4	C3	111.5(3)
N1	N2	C5	111.2(3)	F4	C4	C5	112.3(3)
N1	N2	C9	120.4(3)	F4	C4	C3	113.3(4)
C5	N2	C9	128.0(3)	C5	C4	C3	103.1(3)
N4	N3	C19	105.0(4)	O4	C22	C21	109.5(3)
C7	N1	N2	104.8(3)	O3	C22	O4	125.2(4)
O1	C10	O2	124.1(4)	O3	C22	C21	125.2(4)
O1	C10	C9	125.7(4)	F10	C16	F9	103.7(3)
O2	C10	C9	110.2(4)	F10	C16	C17	112.9(4)
F1	C8	C7	110.3(3)	F10	C16	C15	111.0(3)
F2	C8	F1	106.1(4)	F9	C16	C17	112.6(3)
F2	C8	C7	113.1(4)	F9	C16	C15	113.3(4)
F3	C8	F1	107.1(4)	C17	C16	C15	103.7(3)
F3	C8	F2	106.0(4)	N4	C21	C22	109.5(3)
F3	C8	C7	113.6(4)	C18	C14	C15	104.2(3)
N4	C17	C18	108.2(4)	C18	C14	C13	113.6(4)
N4	C17	C16	139.5(4)	C13	C14	C15	59.0(3)
C18	C17	C16	112.3(3)	N2	C9	C10	110.9(4)
N3	C19	C18	111.3(4)	C16	C15	C14	108.8(4)
N3	C19	C20	120.4(4)	C13	C15	C16	117.2(4)
C18	C19	C20	128.2(4)	C13	C15	C14	60.0(3)
C7	C6	C2	146.1(4)	C4	C3	C2	109.3(3)
C5	C6	C7	103.2(3)	C1	C3	C2	59.3(3)
C5	C6	C2	110.6(3)	C1	C3	C4	116.6(4)
C17	C18	C19	104.0(4)	C3	C1	C2	61.4(3)
C17	C18	C14	111.0(4)	C15	C13	C14	61.0(3)
C19	C18	C14	145.0(4)	O4	C23	C24	107.1(4)
N1	C7	C8	118.8(4)	O2	C11	C12	107.7(4)
N1	C7	C6	112.3(4)	F8	C20	C19	113.5(5)
C6	C7	C8	128.9(3)	F8	C20	F6	111.1(7)
N2	C5	C6	108.5(3)	F8	C20	F7	108.2(7)
N2	C5	C4	138.7(4)	F6	C20	C19	112.2(4)
C6	C5	C4	112.7(3)	F6	C20	F7	99.0(5)
C6	C2	C3	104.1(3)	F7	C20	C19	112.0(4)

Table 4.4.11 Torsion Angles in ° for **C5.11**.

Atom	**Atom**	**Atom**	**Atom**	**Angle/°**	**Atom**	**Atom**	**Atom**	**Atom**	**Angle/°**

F10	C16	C15	C14	118.7(4)	C6	C5	C4	F5	-117.4(4)
F10	C16	C15	C13	-176.0(4)	C6	C5	C4	F4	125.4(4)
F9	C16	C15	C14	-125.2(4)	C6	C5	C4	C3	3.0(5)
F9	C16	C15	C13	-59.9(6)	C6	C2	C3	C4	0.5(5)
F5	C4	C3	C2	119.5(4)	C6	C2	C3	C1	-109.6(4)
F5	C4	C3	C1	-175.9(4)	C6	C2	C1	C3	92.7(4)
F4	C4	C3	C2	-123.6(4)	C18	C17	C16	F10	-117.4(4)
F4	C4	C3	C1	-59.0(5)	C18	C17	C16	F9	125.6(4)
O4	C22	C21	N4	-175.0(4)	C18	C17	C16	C15	2.7(4)
F1	C8	C7	N1	-179.7(4)	C18	C19	C20	F8	-37.1(9)
F1	C8	C7	C6	-0.1(7)	C18	C19	C20	F6	89.7(6)
O3	C22	C21	N4	7.3(6)	C18	C19	C20	F7	-160.0(5)
O1	C10	C9	N2	-0.1(6)	C18	C14	C15	C16	1.9(5)
O2	C10	C9	N2	179.8(3)	C18	C14	C15	C13	-109.3(4)
F2	C8	C7	N1	61.6(6)	C18	C14	C13	C15	92.8(4)
F2	C8	C7	C6	-118.8(5)	C7	C6	C5	N2	-1.5(5)
F3	C8	C7	N1	-59.4(6)	C7	C6	C5	C4	179.2(4)
F3	C8	C7	C6	120.3(6)	C7	C6	C2	C3	177.7(7)
N4	N3	C19	C18	1.1(4)	C7	C6	C2	C1	115.4(7)
N4	N3	C19	C20	178.7(4)	C5	N2	N1	C7	-1.3(5)
N4	C17	C18	C19	-1.7(4)	C5	N2	C9	C10	-91.7(5)
N4	C17	C18	C14	176.3(3)	C5	C6	C7	N1	0.7(5)
N4	C17	C16	F10	65.5(7)	C5	C6	C7	C8	-178.9(5)
N4	C17	C16	F9	-51.5(7)	C5	C6	C2	C3	1.4(5)
N4	C17	C16	C15	-174.3(5)	C5	C6	C2	C1	-60.9(5)
N2	N1	C7	C8	-180.0(4)	C5	C4	C3	C2	-2.0(5)
N2	N1	C7	C6	0.3(5)	C5	C4	C3	C1	62.6(5)

N2	C5	C4	F5	63.7(7)	C2	C6	C7	N1	-175.7(6)
N2	C5	C4	F4	-53.6(7)	C2	C6	C7	C8	4.7(11)
N2	C5	C4	C3	-175.9(6)	C2	C6	C5	N2	176.4(4)
N3	N4	C17	C18	2.6(5)	C2	C6	C5	C4	-2.9(5)
N3	N4	C17	C16	179.7(5)	C4	C3	C1	C2	-97.7(4)
N3	N4	C21	C22	77.6(5)	C22	O4	C23	C24	179.3(4)
N3	C19	C18	C17	0.4(5)	C16	C17	C18	C19	-179.7(3)
N3	C19	C18	C14	-176.4(6)	C16	C17	C18	C14	-1.7(5)
N3	C19	C20	F8	145.7(8)	C16	C15	C13	C14	-97.0(4)
N3	C19	C20	F6	-87.4(6)	C21	N4	N3	C19	-170.7(3)
N3	C19	C20	F7	22.8(6)	C21	N4	C17	C18	169.8(4)
N1	N2	C5	C6	1.8(5)	C21	N4	C17	C16	-13.0(8)
N1	N2	C5	C4	-179.2(5)	C9	N2	N1	C7	-174.4(4)
N1	N2	C9	C10	80.1(5)	C9	N2	C5	C6	174.2(4)
C10	O2	C11	C12	174.7(5)	C9	N2	C5	C4	-6.8(9)
C17	N4	N3	C19	-2.2(4)	C1	C2	C3	C4	110.1(4)
C17	N4	C21	C22	-88.8(5)	C13	C14	C15	C16	111.2(4)
C17	C18	C14	C15	-0.1(5)	C23	O4	C22	O3	1.6(7)
C17	C18	C14	C13	-62.2(5)	C23	O4	C22	C21	-176.1(4)
C17	C16	C15	C14	-2.7(4)	C11	O2	C10	O1	2.5(6)
C17	C16	C15	C13	62.5(5)	C11	O2	C10	C9	-177.4(4)
C19	C18	C14	C15	176.6(6)	C20	C19	C18	C17	-177.0(4)
C19	C18	C14	C13	114.5(7)	C20	C19	C18	C14	6.2(9)

Table 4.4.12 Hydrogen Fractional Atomic Coordinates ($\times 10^4$) and Equivalent Isotropic Displacement Parameters ($Å^2 \times 10^3$) for **C5.11**. U_{eq} is defined as 1/3 of the trace of the orthogonalised U_{ij}.

Atom	**x**	**y**	**z**	U_{eq}
H2	6814.7	4023.44	7418.27	35
H21A	2694.81	-737.17	5429.06	36
H21B	1370.21	280.54	6307.04	36

Atom	x	y	z	U_{eq}
H14	2663.18	6091.2	2729.1	37
H9A	7839.13	10814.12	4715.05	38
H9B	6805.04	9845.9	3795.67	38
H15	304.54	6053.39	4778.09	37
H3	5247.12	4144.6	5218.01	39
H1A	3751.38	4310.79	7638.33	43
H1B	3982.84	6168.01	7388.76	43
H13A	-297.75	5994.4	2285.12	44
H13B	-197.8	4126.16	2515.23	44
H23A	4412.48	278.63	9554.23	44
H23B	5884.28	-578.24	8652.45	44
H11A	10842.07	9777.05	625.66	45
H11B	11888.25	10860.02	1429.63	45
H24A	4674.65	-2920.08	9656.74	71
H24B	3193.48	-2073.91	10542.68	71
H24C	5054.01	-1999.04	10949.33	71
H12A	9536.57	11899.75	-510.06	97
H12B	11514.77	11990.42	-934.49	97
H12C	10615.97	12967.33	269.97	97

4.5 Acquisition methods, retention times, chromatograms, and MS spectra

4.5.1 LenC-1 (GC-MS)

Structures & IDs:

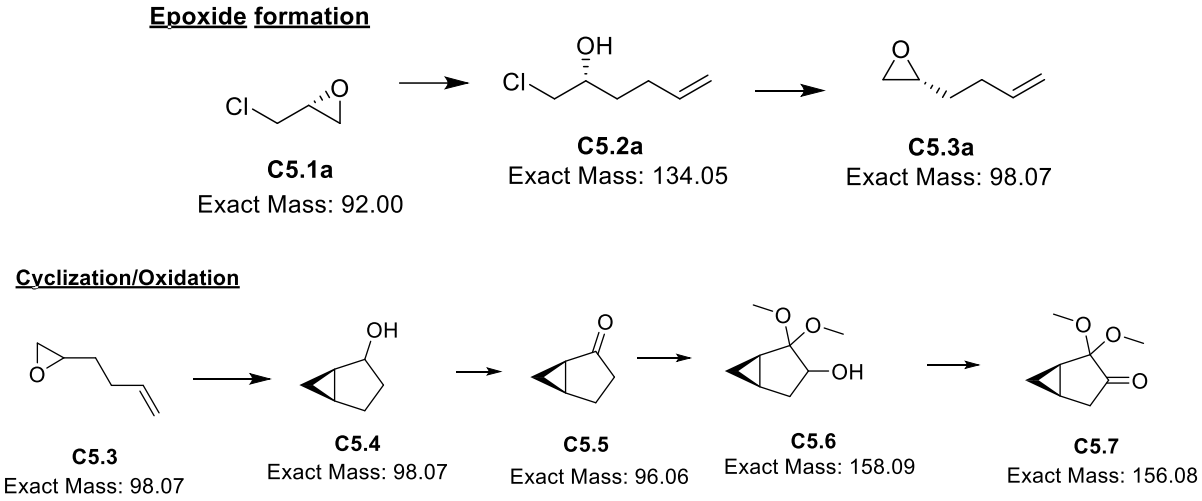

Instrument Type: Agilent 6890 gas chromatograph (GC) with a 5977 mass spectrometer detector (MSD)

Conditions:
Column: J&W HP-1 GC Column, 30 m, 0.32 mm, 5.00 µm, 5 inch cage

Inlet Pressure: 7.87 psi | Split Ratio: 50 : 1 | Split Flow: 70 mL/min
Column flow: 1.4 mL/min | Injection Temp: 250 ºC | Injection volume: 1 µL
Total Flow: 74.11 mL/min | Solvent Delay: 3.5 min | Runtime: 15 min

Temperature Program:

Time (min)	Ramp (˚C/min)	Temp (°C)	Hold (min)
Initial	-	50	3
-	25	225	5

MS Parameters:

Transfer Line Temp (˚C)	250
Source Temp (˚C)	230
Quad Temp (˚C)	150
Electron Energy (eV)	70
Mass Range	30-1000

Sample preparation:
Prepare solutions at approximately 0.5 - 1 mg/mL in acetonitrile. **C5.3** is quite volatile and must be prepared carefully for quantitation.

Retention Times

Compound	*m/z*	Time (min)
C5.1a	62, 57	6.35
C5.3	97, 67	7.28
C5.4	97	8.37
C5.5	96	8.86
C5.2	116, 81	9.16
C5.7	128, 125	10.60
C5.6	141, 117, 88	10.72

Representative Chromatograms
C5.1a – C5.3

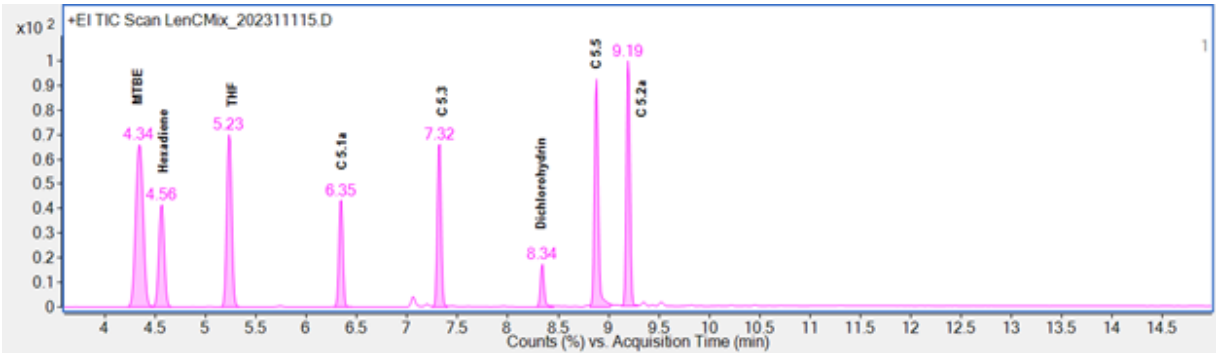

C5.4 and C5.5

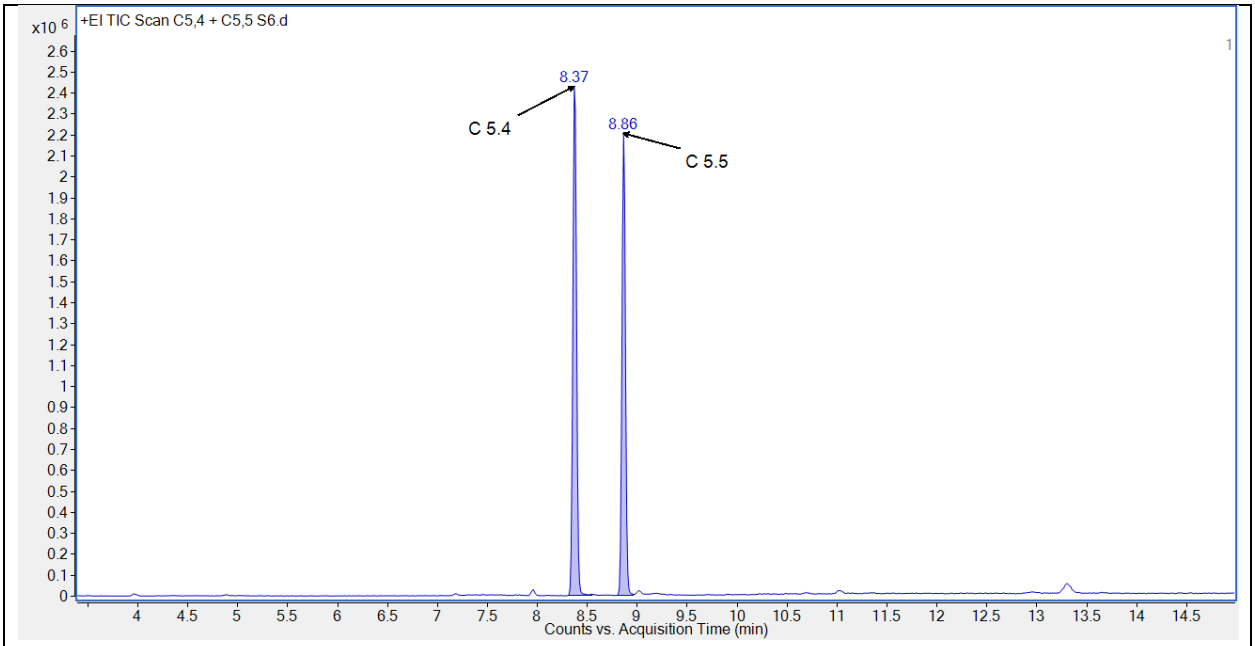

C5.6 and C5.7

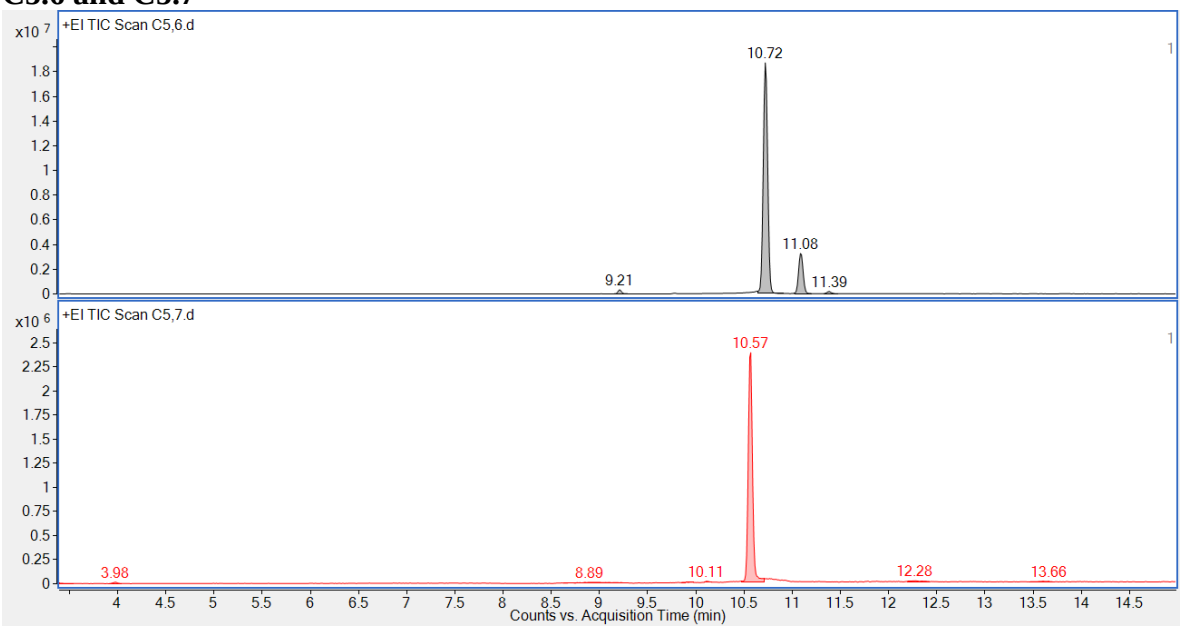

Mass spectra:

C5.1a

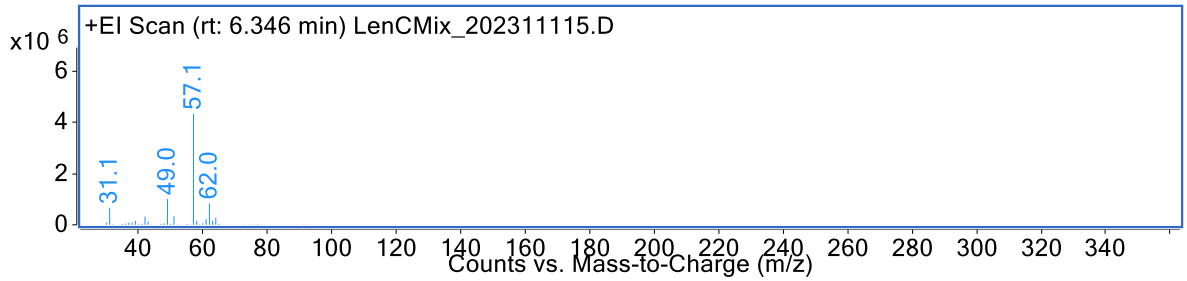

C5.2

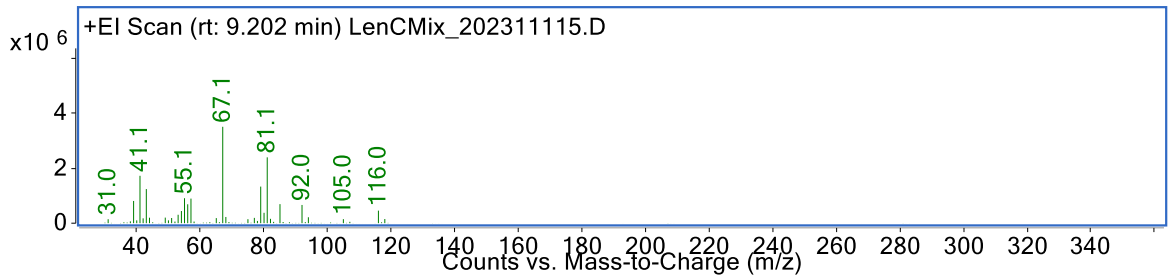

C5.3

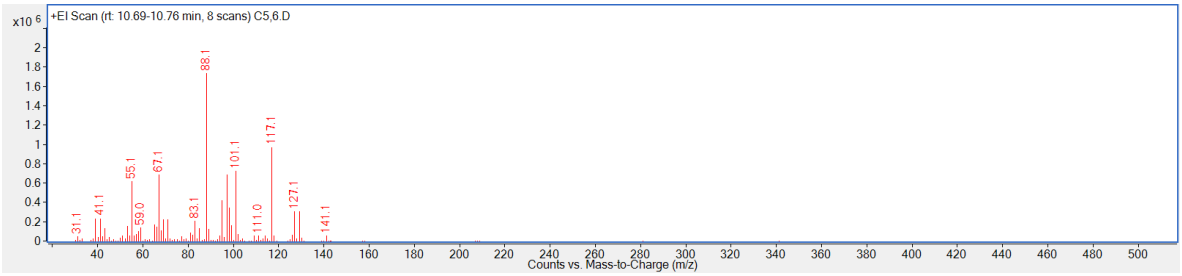

C5.4

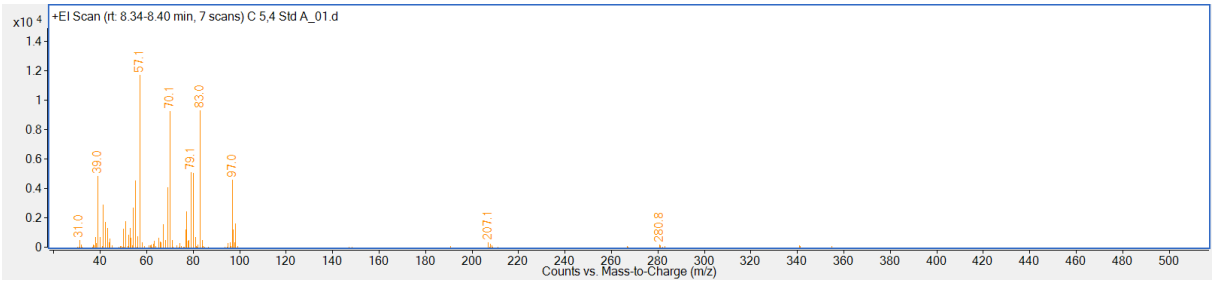

C5.5

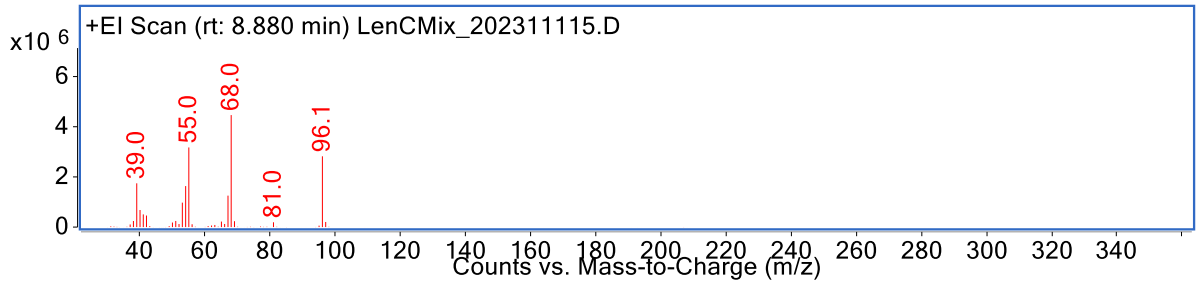

C5.6

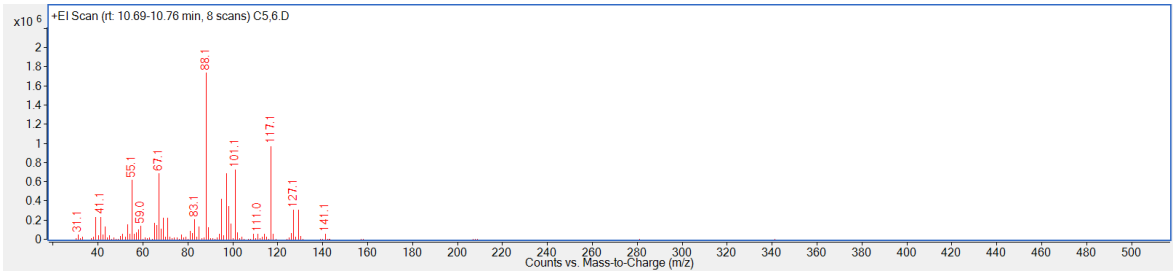

C5.7

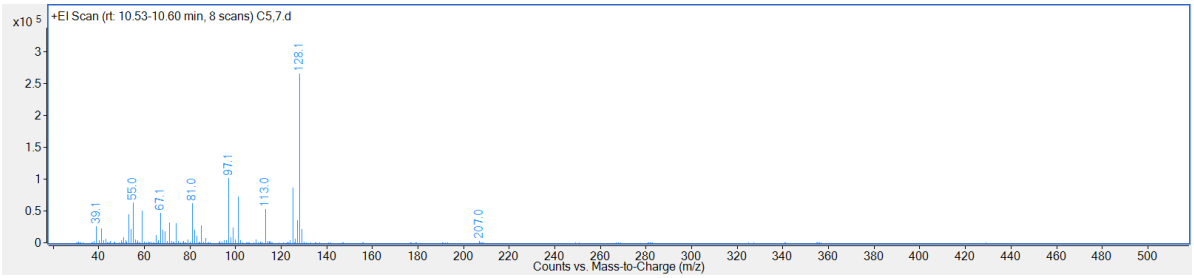

4.5.2 LenC-2 (GC-MS)

Structures & IDs:

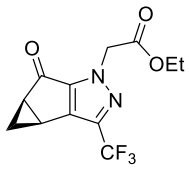

C5.9
Exact Mass: 288.07

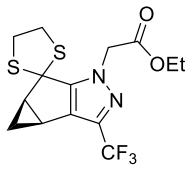

C5.10
Exact Mass: 364.05

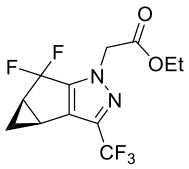

C5.11
Exact Mass: 310.07

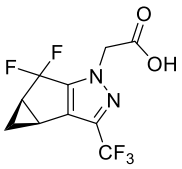

Frag C
Exact Mass: 282.04

Instrument Type: Agilent 8890 gas chromatograph (GC) with a 5977 mass spectrometer detector (MSD)

Conditions:
Column: J&W HP-5ms GC Column, 30 m, 0.25 mm, 0.25 µm

Inlet Pressure: 12.432 psi | Split Ratio: 50 : 1 | Split Flow: 70 mL/min
Column flow: 1.4 mL/min | Injection Temp: 250 ºC | Injection volume: 1 µL
Total Flow: 74.11 mL/min | Solvent Delay: 2.0 min | Runtime: 14.0 min

Temperature Program:

Time (min)	Ramp (˚C/min)	Temp (°C)	Hold (min)
Initial	-	50	3
-	25	250	3

MS Parameters:

Transfer Line Temp (˚C)	250
Source Temp (˚C)	230
Quad Temp (˚C)	150
Electron Energy (eV)	70
Mass Range	40-1000

Sample preparation:
Prepare solutions at approximately 0.5 - 1 mg/mL in methanol.

Retention Times

Compound	*m/z*	Time (min)
C5.11	310, 291, 237	9.24
Frag C	282, 237	9.65
C5.9	288, 242, 215	10.20
C 5.10	364, 262, 231	13.27

Representative Chromatograms

C5.9

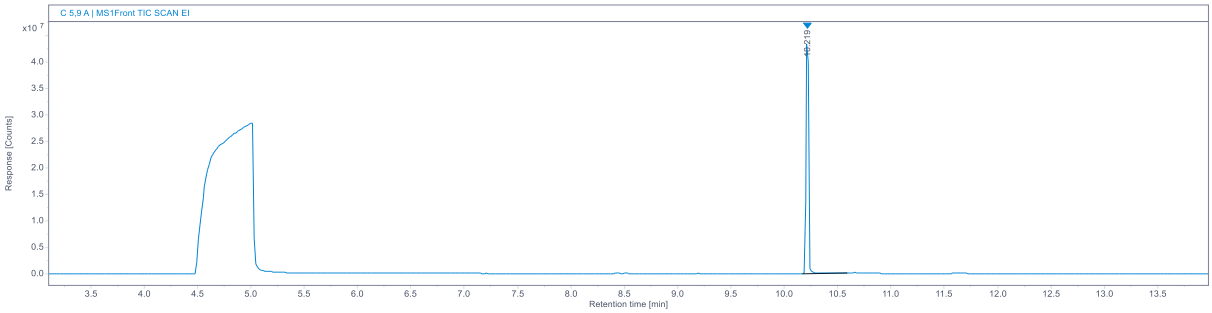

C5.10

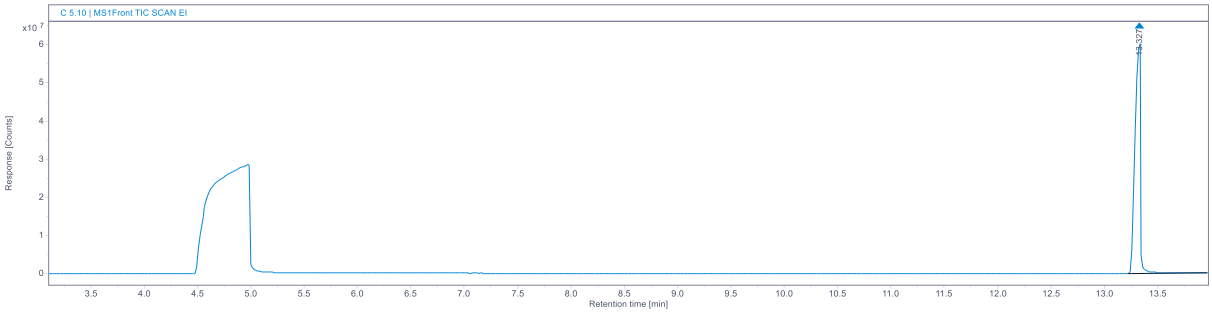

C5.11

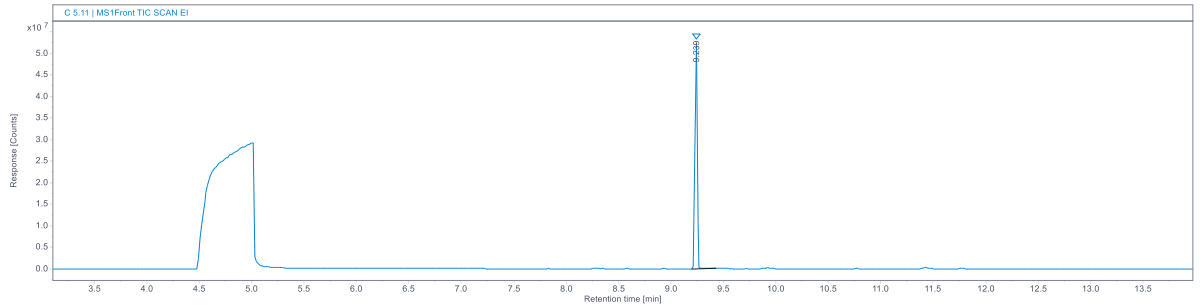

Frag C

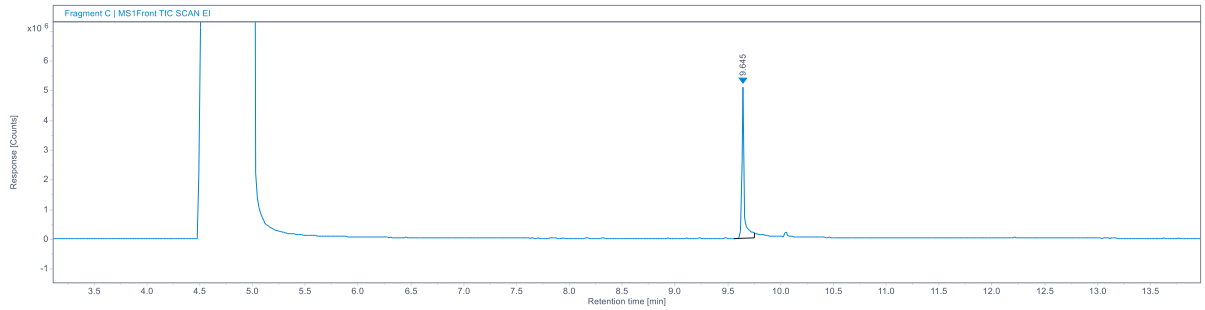

Mass spectra

C5.9

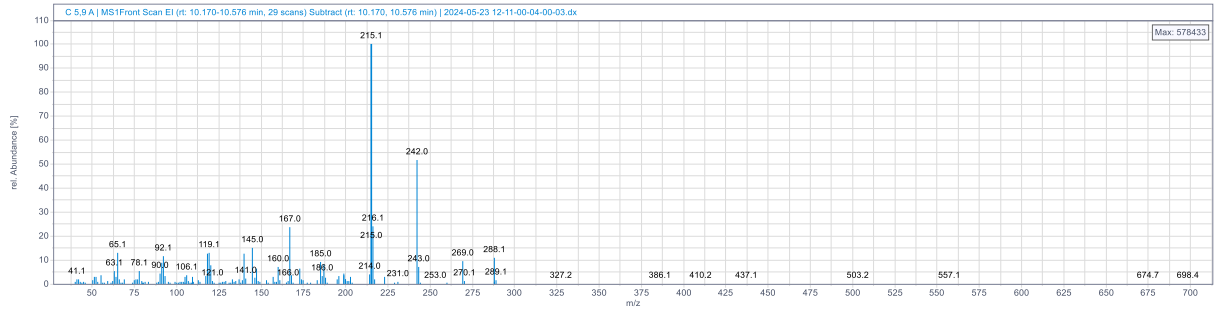

C5.10

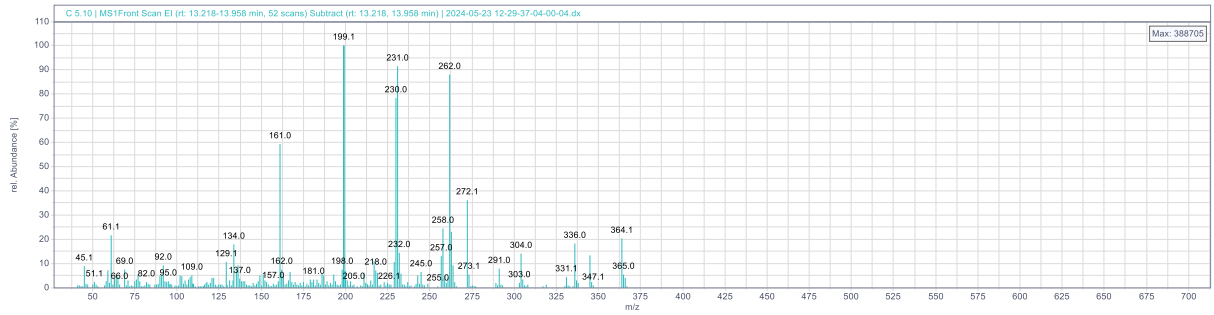

C5.11

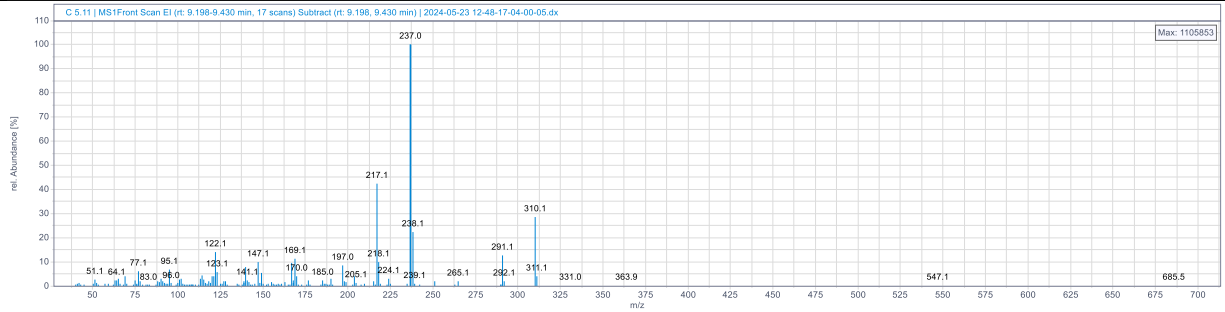

Frag C

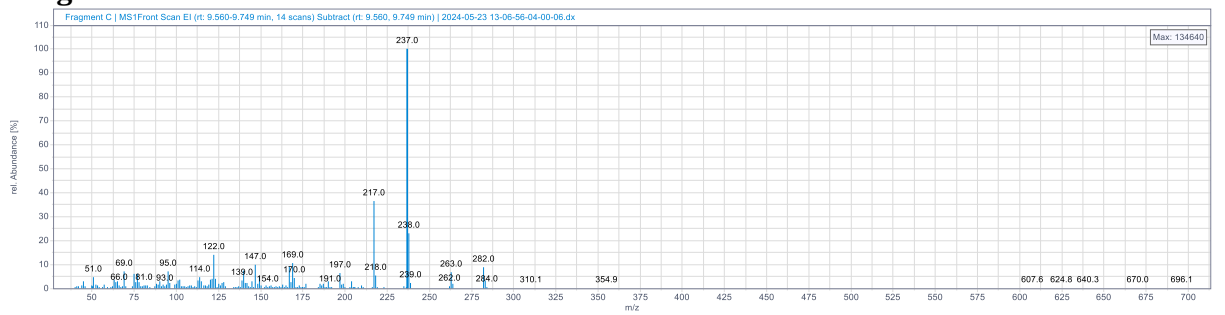

4.5.3 LenC-3 (Chiral, GC-FID)

Structures & IDs:

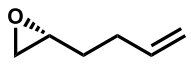

C5.3 - (R) Enantiomer
Exact Mass: 98.07

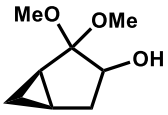

C5.6
Exact Mass: 158.09

Instrument Type: Agilent 6890 gas chromatograph (GC) with a flame ionization detector (FID)

Conditions:

Column: RT-GammaDEXsa (30 m x 0.25 mm x 0.25 µm)

Inlet Pressure: 16.4 psi
Split Ratio: 50 : 1
Split Flow: 71.3 mL/min
Column flow: 1.4 mL/min
Inlet Temp: 250°C
Injection volume: 1 µL
Runtime: 16 min
FID Gas Flows:
H_2 = 35.0 mL/min
Air = 450 mL
Makeup (N_2) = 30.0 mL/min

Temperature Program: Isothermal at 60 °C
FID Temperature: 250 °C

Sample preparation: Prepare solutions at approximately 5.0 mg/mL in methanol.

Retention Times	
Compound	**Time (min)**
C5.6 Enantiomer 1	4.36
C5.6 Enantiomer 2	4.63
C5.3 (R) enantiomer	12.48
C5.3 (S) enantiomer	13.19

Notes: For accurate integration for **C5.3**, draw through the entire tail of the (R) peak and tangent skim the (S) peak.

Representative Chromatograms

C5.3

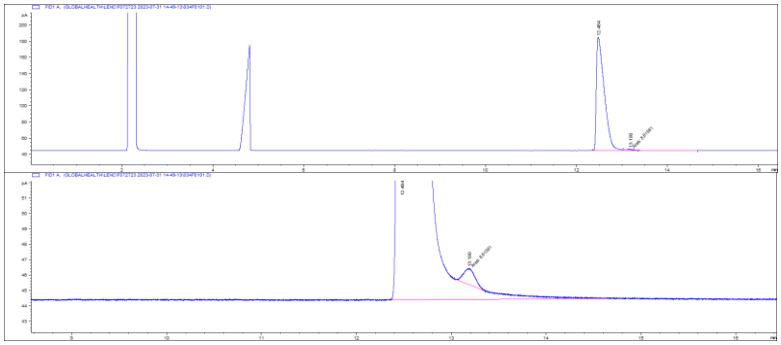

C5.6

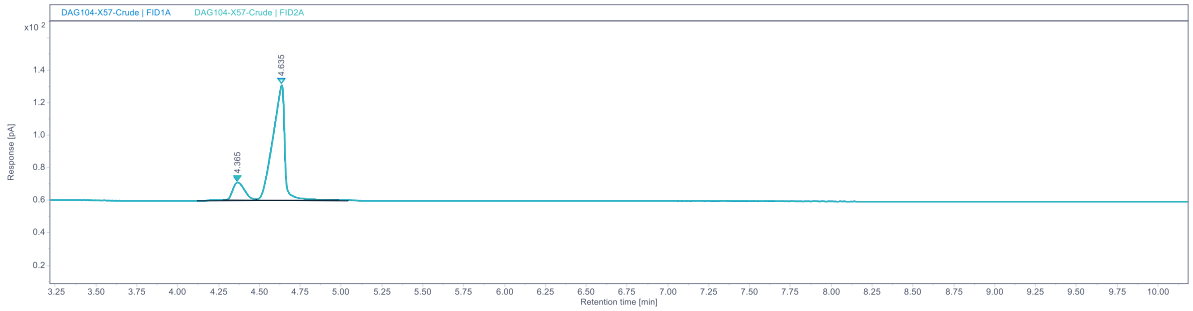

4.5.4 LenC-4 (Chiral, GC-MS)

Structures & IDs:

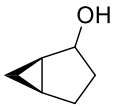

C5.4
Exact Mass: 98.07

Instrument Type: Agilent 6890 gas chromatograph (GC) with a 5977 mass spectrometer detector (MSD)

Conditions:

Column: J&W HP-1 GC Column, 30 m, 0.32 mm, 5.00 µm, 5 inch cage

Inlet Pressure: 7.87 psi | Split Ratio: 50 : 1 | Split Flow: 70 mL/min

Column flow: 1.4 mL/min | Injection Temp: 250 °C | Injection volume: 1 µL

Total Flow: 74.11 mL/min | Solvent Delay: 3.5 min | Runtime: 15 min

Temperature Program:

Time (min)	Ramp (°C/min)	Temp (°C)	Hold (min)
Initial	-	50	3
-	25	225	5

MS Parameters:

Transfer Line Temp (°C)	250
Source Temp (°C)	230
Quad Temp (°C)	150
Electron Energy (eV)	70
Mass Range	30-1000

Sample preparation:

Prepare solutions at approximately 0.5 - 1 mg/mL in acetonitrile.

Retention Times

Compound	Time (min)
C5.4 (R) enantiomer	8.37
C5.4 (S) enantiomer	8.49

Representative Chromatograms

C5.4

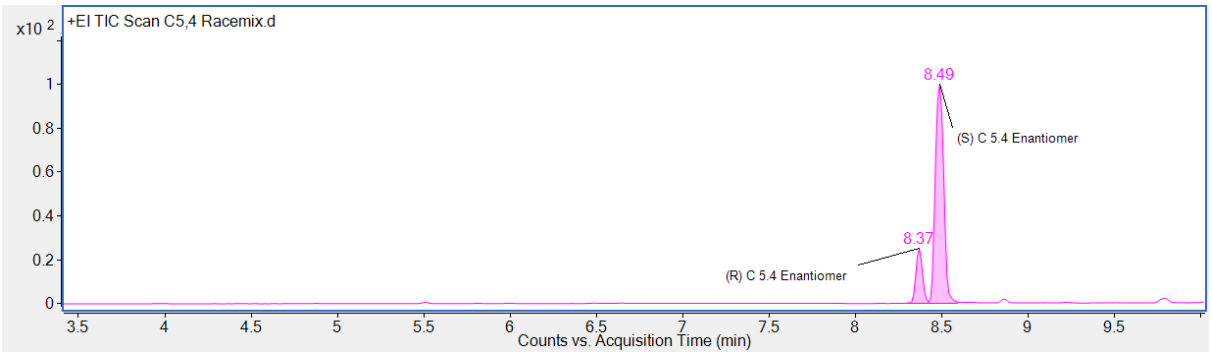

4.5.5 LenC-5 (Chiral, GC-FID)

Structures & IDs:

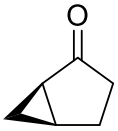

C5.5

Exact Mass: 96.06

Instrument Type: Agilent 6890 gas chromatograph (GC) with a flame ionization detector (FID)

Conditions:

Column: RT-GammaDEXsa (30 m x 0.25 mm x 0.25 µm)

Inlet Pressure: 10.0 psi | Split Ratio: 50 : 1 | Split Flow: 27.8 mL/min

Column flow: 0.56 mL/min | Inlet Temp: 200°C | Injection volume: 1 µL

Runtime: 45 min

Temperature Program: Isothermal at 125 °C

FID Temperature: 200 °C

FID Gas Flows:

H_2 = 35.0 mL/min

Air = 450 mL

Makeup (N_2) = 30.0 mL/min

Sample preparation: Dilute samples in MeCN

Retention Times

Compound	Time (min)
C5.5 Enantiomer 1	19.48
C5.5 Enantiomer 2	20.96

Notes: Stereochemical assignments unknown

Representative Chromatogram

C5.5

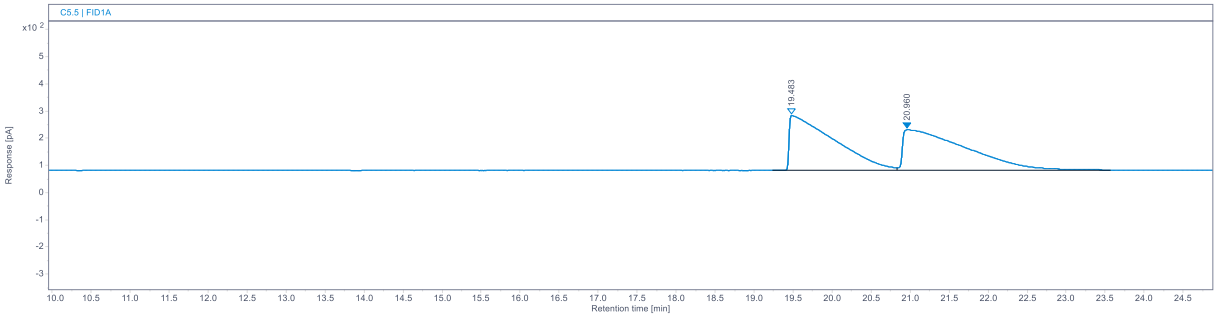

4.5.6 LenC-6 (Chiral, SFC-DAD)

Structures & IDs:

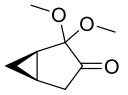

C5.7
Exact Mass: 156.08

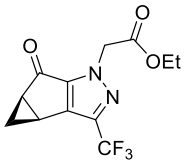

C5.9
Exact Mass: 288.07

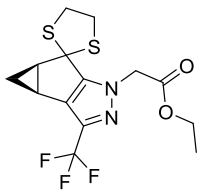

C5.10
Exact Mass: 364.05

Instrument Type: Agilent 1260 super critical fluid chromatograph (SFC) with diode array detector (DAD)

Conditions:

Column: ChiralPak IG-3 4.6x250mm; 3 µm

Mobile Phase A: CO_2

Mobile Phase B: Methanol

Injection volume: 1 µL Column temp: 25°C Flow rate: 2.0 mL/min

BPR Pressure: 100 bar BPR Temp: 60 °C

Detector wavelength(s): 210 nm

LC Gradient Table:

Time (min)	%A	%B
0.0	95	5
10.0	95	5

Sample preparation:

Prepare solution in methanol at approximately 5 mg/mL.

Retention Times

Compound	Time (min)
C5.7 Enantiomer 1	2.78
C5.7 Enantiomer 2	3.01
C5.9 Enantiomer 1	2.31
C5.9 Enantiomer 2	2.55
C5.10 Enantiomer 1	5.14
C5.10 Enantiomer 2	6.56

Notes: Stereochemical assignments unknown

Representative Chromatograms

C5.7

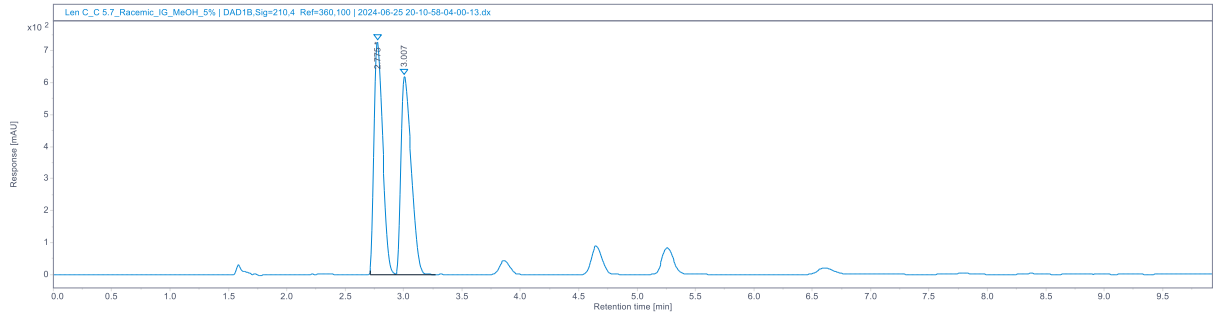

C5.9

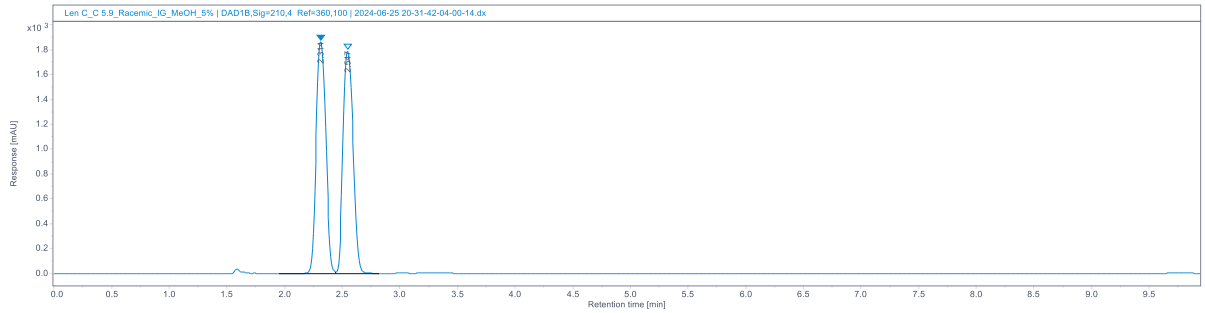

C5.10

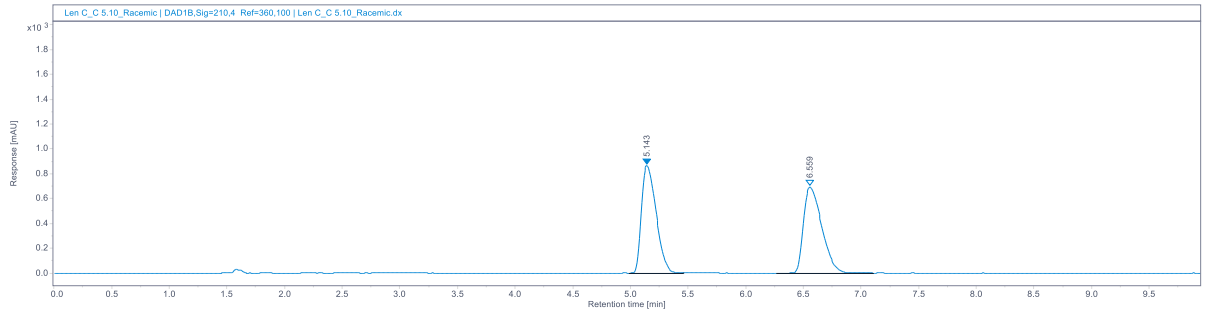

UV Spectra

C5.7

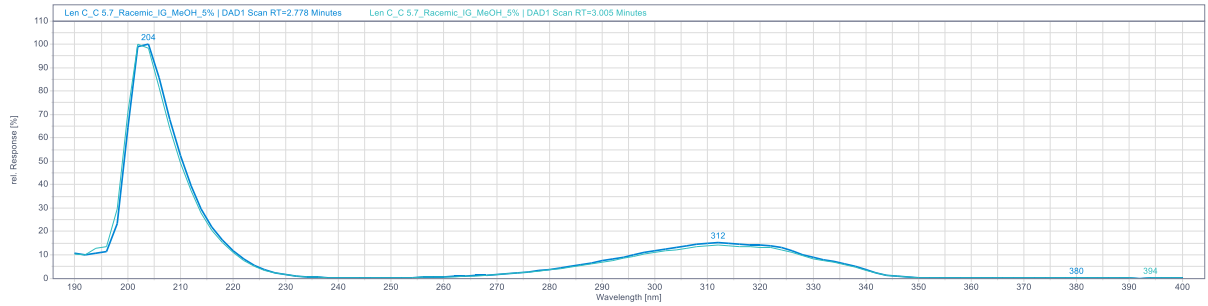

C5.9

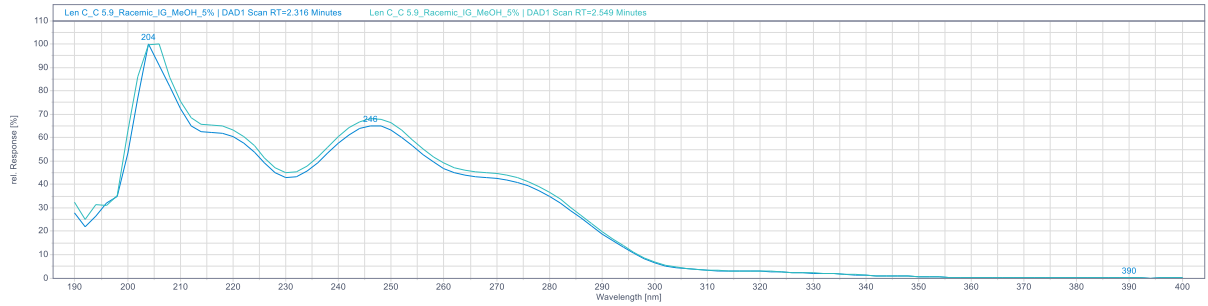

C5.10

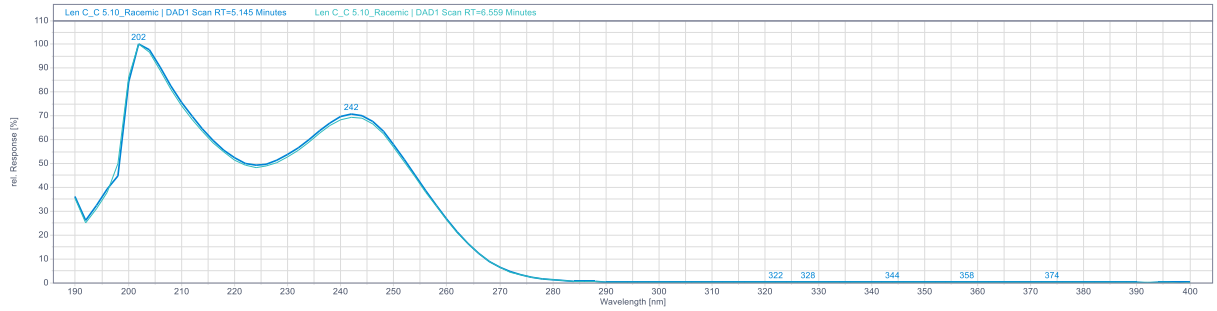

4.5.7 LenC-7 (Chiral, SFC-DAD)

Structures & IDs:

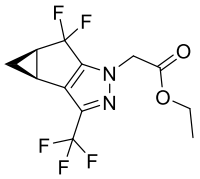

Exact Mass: 310.07

C5.11

Instrument Type: Agilent 1260 super critical fluid chromatograph (SFC) with diode array detector (DAD)

Conditions:

Column: ChiralPak IG-3 4.6x250mm; 3 µm

Mobile Phase A: CO_2

Mobile Phase B: Acetonitrile

Injection volume: 1 µL

Column temp: 25°C

Flow rate: 2.0 mL/min

BPR Pressure: 100 bar

BPR Temp: 60 °C

Detector wavelength(s): 240 nm

LC Gradient Table:

Time (min)	%A	%B
0.0	80	20
6.0	80	20

Post-run equilibration: None

Sample preparation:

Prepare solution in acetonitrile at ~1.0 mg/mL

Retention Times

Compound	Time (min)
C5.11 Undesired enantiomer	2.18
C5.11 Desired enantiomer (S,R)	2.54

Representative Chromatograms

C5.11 Racemic

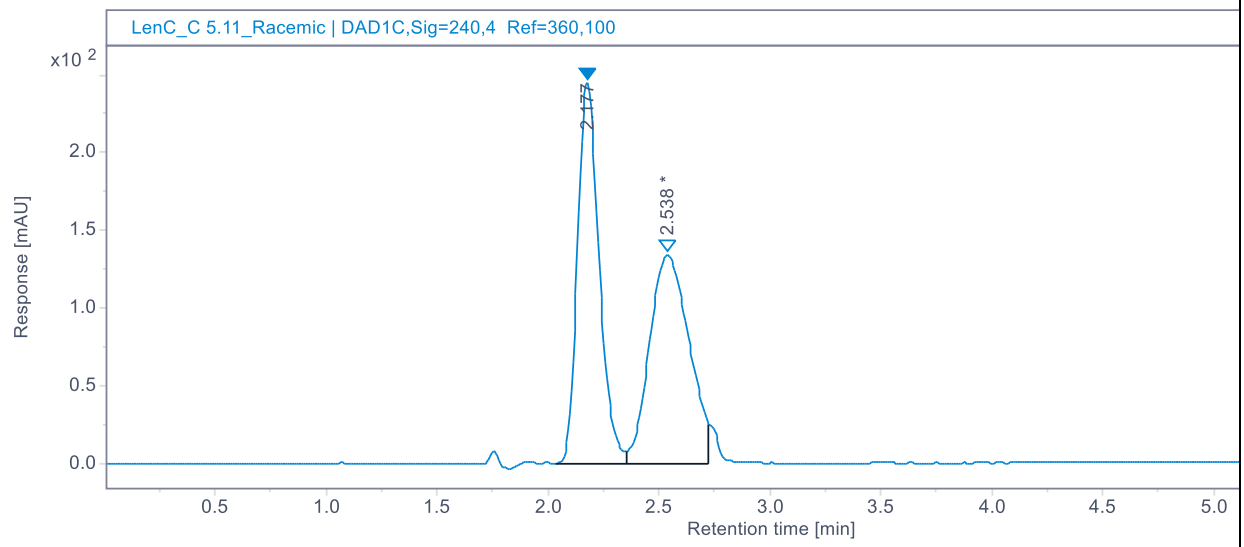

C5.11 Enantiopure

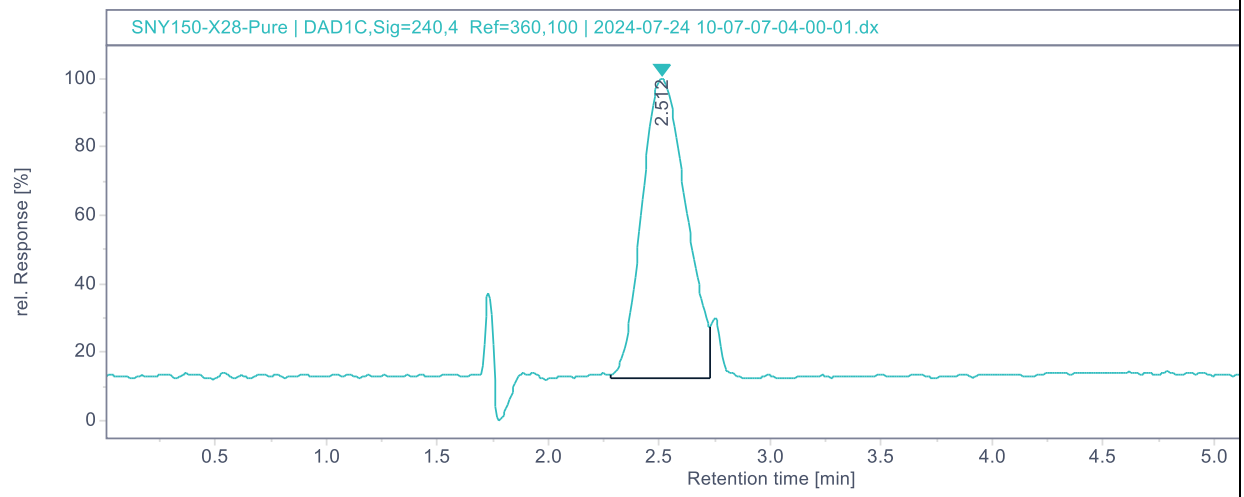

**Peak shoulder at 2.7 min is related to sample solvent (present in the blank)*

UV Spectra

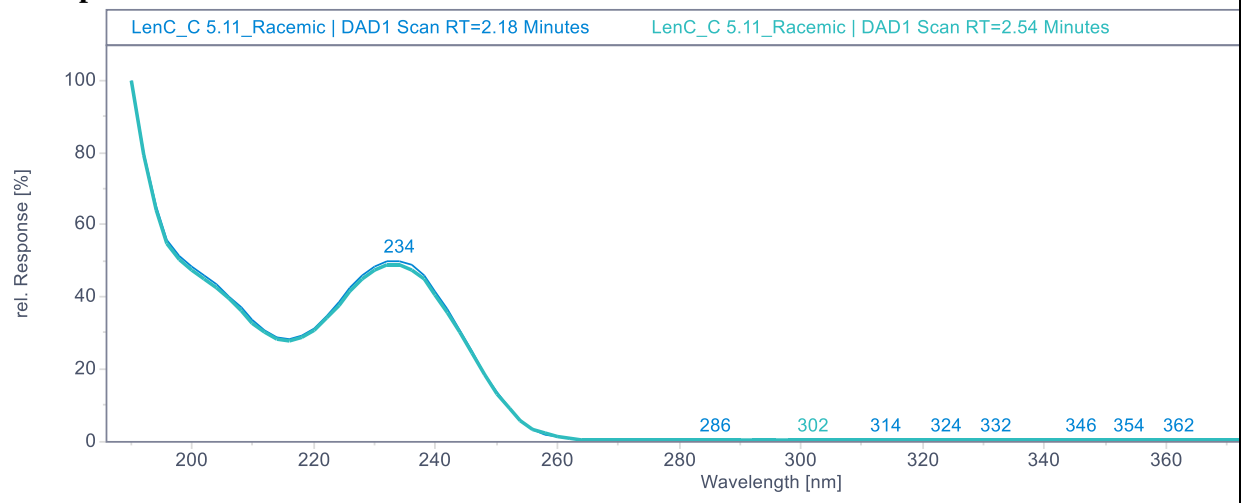

4.5.8 LenC-8 (Chiral, SFC-DAD)

Structures & IDs:

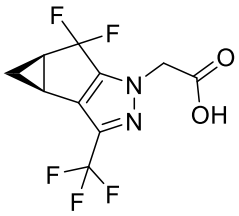

Frag C

Exact Mass: 282.04

Instrument Type: Agilent 1260 super critical fluid chromatograph (SFC) with diode array detector (DAD)

Conditions:

Column: ChiralPak IC-3 4.6x250mm; 3 µm

Mobile Phase A: CO_2

Mobile Phase B: Isopropanol (0.05% DEA)

Injection volume: 1 µL

Column temp: 25ºC

Flow rate: 2.35 mL/min

BPR Pressure: 100 bar

BPR Temp: 60 °C

Detector wavelength(s): 240 nm

LC Gradient Table:

Time (min)	%A	%B
0.0	80	20
12.0	80	20

Sample preparation:

Prepare solution in methanol at approximately 10 mg/mL

Retention Times	
Compound	**Time (min)**
Frag C Enantiomer 1	3.53
Frag C Enantiomer 2	8.52
Notes: Stereochemical assignments unknown	

Representative Chromatogram

Frag C

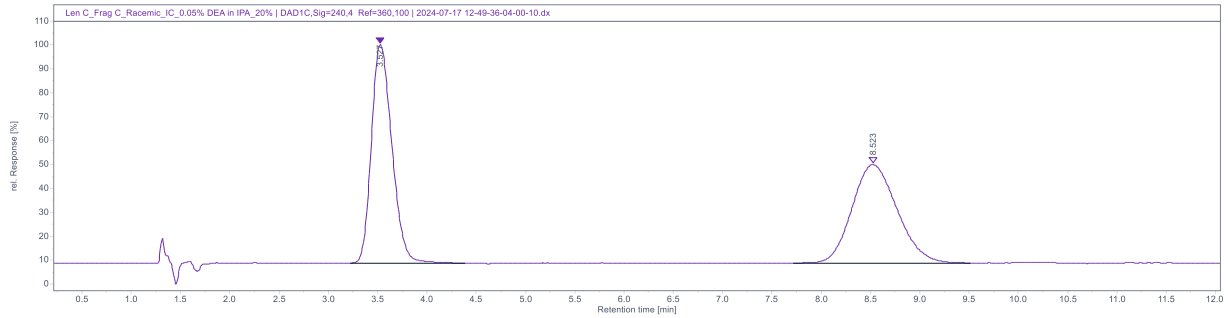

UV Spectra

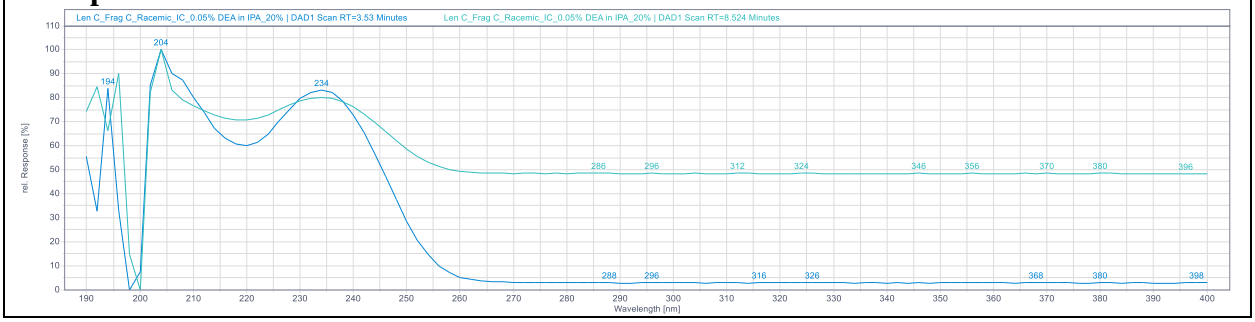

4.6 Acronyms

AIDS	acquired immunodeficiency syndrome
ART	antiretroviral therapy
ATR	attenuated total reflection
ARVs	antiretroviral medications
A%	area percent
Ac_2O	acetic anhydride
AcOH	acetic acid
Å	angstrom
BMGF	Bill and Melinda Gates Foundation
$BF_3{\cdot}OEt_2$	boron trifluoride diethyl etherate
BAST	bis(2-methoxyethyl)aminosulfur trifluoride (Deoxo-Fluor®)
CF_3CO_2Et	ethyl trifluoroacetate
DCM	dichloromethane
DMSO	dimethyl sulfoxide

DMF	dimethylformamide
DIPEA	*N*,*N*-diisopropylethylamine
DMP	Dess-Martin periodinane
DSC	differential scanning calorimetry
DFI	2,2-difluoro-1,3-dimethylimidazolidine
DBDMH	1,3-dibromo-5,5-Dimethylhydantoin
DMAP	4-Dimethylaminopyridine
EtOAc	ethyl acetate
EAG/HCl	ethyl amino glycinate hydrochloride
ESI	electrospray ionization
EtOH	ethyl alcohol
1,2-EDT	ethane-1,2-dithiol
Frag A	(S)-1-(3,6-dibromopyridin-2-yl)-2-(3,5-difluorophenyl)ethan-1-amine
Frag B	4-chloro-7-(4,4,5,5-tetramethyl-1,3,2-dioxaborolan-2-yl)-1-(2,2,2-trifluoroethyl)-1H-indazol-3-amine
Frag C	2-((3bS,4aR)-5,5-difluoro-3-(trifluoromethyl)-3b,4,4a,5-tetrahydro-1H-cyclopropa[3,4]cyclopenta[1,2-c]pyrazol-1-yl)acetic acid
Fluolead	4-tert-butyl-2,6-dimethylphenylsulfur Trifluoride
FID	flame-ionization detector
FDA	food and drug administration
GCMS-TIC	gas chromatography-mass spectrometry total ion chromatogram
HIV	human immunodeficiency virus
HDP	high-density polyethylene (HDPE)
HRMS	high-resolution mass spectrometry
HF-Py	Hydrogen fluoride pyridine (Olah's reagent)
i-PrOAc	isopropyl acetate
i-PrOH	isopropyl alcohol
i-PrMgCl·LiCl	isopropyl magnesium chloride lithium chloride complex
IPC	in-process control
IR	infrared spectroscopy
KOtBu	potassium *tert*-butoxide
LiHMDS	lithium hexamethyldisilazide (Lithium bis(trimethylsilyl)amide)
LenC	Lenacapavir Fragment C
LCMS	liquid chromatography–mass spectrometry
LiTMP	Lithium 2,2,6,6-tetramethylpiperidide
M4ALL	Medicines for All Institute
MTBE	methyl tert-butyl ether
Me_4NF	tetrabutylammonium fluoride
MS-EI	mass spectrometry – electron ionization
m/z	mass/charge
MS-DART	Direct Analysis in Real-Time Mass Spectrometry
MsOH	methanesulfonic acid
MDR HIV	multidrug-resistant HIV

NBS	*N*-bromosuccinimide
NMR	Nuclear Magnetic Resonance
NMO	*N*-methylmorpholine *N*-oxide
n-PrOH	*n*-propanol
OPT	scale-up optimization
OXONE	potassium peroxymonosulfate ($2KHSO_5 \cdot KHSO_4 \cdot K_2SO_4$)
PDR	process development report
PrEP	pre-exposure prophylaxis
PMI	process mass intensity
PPE	personal protective equipment
PTFE	polytetrafluoroethylene
PMA	phosphomolybdic acid
PIDA	(Diacetoxyiodo)benzene, phenyl iodine(III) diacetate, $PhI(OAc)_2$
qNMR	quantitative Nuclear Magnetic Resonance
rac	racemic
RMC	raw material cost
SDS	safety data sheet
SRS	synthetic route scouting
SFC	Supercritical fluid chromatography
SOP	Standard Operating Procedure
SO_2F_2	sulfuryl fluoride
TLC	thin-layer chromatography
TBS-Cl	*tert*-butyldimethylsilyl chloride
TC	treatment cost
TCCA	trichloroisocyanuric acid
TE	techno-economic
TEMPO	2,2,6,6-Tetramethylpiperidine-1-oxyl
TMP	2,2,6,6-tetramethylpiperidine
THF	tetrahydrofuran
TFA	trifluoroacetic acid
TFAA	trifluoroacetic anhydride
TEA	triethylamine
TfOH	triflic acid
TMP-MgCl·LiCl	2,2,6,6-tetramethylpiperidinylmagnesium chloride lithium chloride complex solution
TPAP	tetrapropylammonium perruthenate
UV	ultraviolet
V	volume
ν max	wavenumber
Xtalfluor-E	DAST difluorosulfinium salt, (Diethylamino)difluorosulfonium tetrafluoroborate
$[\alpha]_D^{20}$	specific rotation

5 Acknowledgements

This work was supported with funding from BMGF. M4ALL would like to express our gratitude to Dr. Trevor Laird, Dr. John Dillon, Dr. Ryan Nelson (BMGF), and Dr. Mark Krook for their helpful technical guidance throughout this project, as well as Silpa Sundaram (BMGF), Dr. Susan Hershenson (BMGF), Dr. John Walker (BMGF) and Scott Rosenblum (BMGF) for the ongoing collaboration and support of the M4ALL mission. The authors thank Dr. Saeed Ahmad and his team for their boundless effort in TE analysis. We also would like to thank Dr. B. Frank Gupton, Dr. Douglas Klumpp, Dr. G. Michael Laidlaw, Dr. Charles Shanahan, Michael Osberg, and Sarah Cox for their input on this work.

6 References

(1) Chun, H. M.; Dirlikov, E.; Cox, M. H.; Sherlock, M. W.; Obeng-Aduasare, Y.; Sato, K.; Voetsch, A. C.; Ater, A. D.; Romano, E. R.; Tomlinson, H.; Modi, S.; Achrekar, A.; Nkengasong, J.; CDC Global HIV Working Group; CDC Global HIV Working Group; Agolory, S.; Amann, J.; Baack, B.; Behel, S.; Date, A.; Hanson, J.; Killam, W. P.; Patel, H.; Patel, S.; Pati, R.; Porter, L.; Warner, A.; Wuhib, T.; Zeh, C.; Faria E Silva Santelli, A. C.; Guevara, G.; Morales, R. E.; Ekra, A. K.; Kitenge, F.; Bonilla, L.; Mazibuko, S.; Damena, T.; Joseph, P.; Upadhyaya, S.; Aitmagambetova, I.; Mwangi, J.; Usmanova, N.; Xaymounvong, D.; Asiimwe, M.; Alice, M.; Masamha, G. J.; Mutandi, G.; Odafe, S.; Romel, L.; Musoni, C.; Mogashoa, M.; Bolo, A.; Nabidzhonov, A.; Mgomella, G.; Lolekha, R.; Alamo-Talisuna, S.; Podolchak, N.; Nguyen, C. K.; Quaye, S.; Mwila, A.; Nyika, P. *Vital Signs* : Progress Toward Eliminating HIV as a Global Public Health Threat Through Scale-Up of Antiretroviral Therapy and Health System Strengthening Supported by the U.S. President's Emergency Plan for AIDS Relief — Worldwide, 2004–2022. *MMWR Morb. Mortal. Wkly. Rep.* **2023**, *72* (12), 317–324. https://doi.org/10.15585/mmwr.mm7212e1.

(2) Phillips, A. N.; Venter, F.; Havlir, D.; Pozniak, A.; Kuritzkes, D.; Wensing, A.; Lundgren, J. D.; De Luca, A.; Pillay, D.; Mellors, J.; Cambiano, V.; Bansi-Matharu, L.; Nakagawa, F.; Kalua, T.; Jahn, A.; Apollo, T.; Mugurungi, O.; Clayden, P.; Gupta, R. K.; Barnabas, R.; Revill, P.; Cohn, J.; Bertagnolio, S.; Calmy, A. Risks and Benefits of Dolutegravir-Based Antiretroviral Drug Regimens in Sub-Saharan Africa: A Modelling Study. *Lancet HIV* **2019**, *6* (2), e116–e127. https://doi.org/10.1016/S2352-3018(18)30317-5.

(3) Margot, N. A.; Naik, V.; VanderVeen, L.; Anoshchenko, O.; Singh, R.; Dvory-Sobol, H.; Rhee, M. S.; Callebaut, C. Resistance Analyses in Highly Treatment-Experienced People With Human Immunodeficiency Virus (HIV) Treated With the Novel Capsid HIV Inhibitor Lenacapavir. *J. Infect. Dis.* **2022**, *226* (11), 1985–1991. https://doi.org/10.1093/infdis/jiac364.

(4) Dvory-Sobol, H.; Shaik, N.; Callebaut, C.; Rhee, M. S. Lenacapavir: A First-in-Class HIV-1 Capsid Inhibitor. *Curr. Opin. HIV AIDS* **2022**, *17* (1), 15–21. https://doi.org/10.1097/COH.0000000000000713.
(5) Bester, S. M.; Wei, G.; Zhao, H.; Adu-Ampratwum, D.; Iqbal, N.; Courouble, V. V.; Francis, A. C.; Annamalai, A. S.; Singh, P. K.; Shkriabai, N.; Van Blerkom, P.; Morrison, J.; Poeschla, E. M.; Engelman, A. N.; Melikyan, G. B.; Griffin, P. R.; Fuchs, J. R.; Asturias, F. J.; Kvaratskhelia, M. Structural and Mechanistic Bases for a Potent HIV-1 Capsid Inhibitor. *Science* **2020**, *370* (6514), 360–364. https://doi.org/10.1126/science.abb4808.
(6) Zhang, J.-Y.; Wang, Y.-T.; Sun, L.; Wang, S.-Q.; Chen, Z.-S. Synthesis and Clinical Application of New Drugs Approved by FDA in 2022. *Mol. Biomed.* **2023**, *4* (1), 26. https://doi.org/10.1186/s43556-023-00138-y.
(7) Zhuang, S.; Torbett, B. E. Interactions of HIV-1 Capsid with Host Factors and Their Implications for Developing Novel Therapeutics. *Viruses* **2021**, *13* (3), 417. https://doi.org/10.3390/v13030417.
(8) Margot, N.; Ram, R.; Rhee, M.; Callebaut, C. Absence of Lenacapavir (GS-6207) Phenotypic Resistance in HIV Gag Cleavage Site Mutants and in Isolates with Resistance to Existing Drug Classes. *Antimicrob. Agents Chemother.* **2021**, *65* (3), e02057-20. https://doi.org/10.1128/AAC.02057-20.
(9) Guinle, M. I. B. A New Way to Prevent HIV Delivers Dramatic Results in Trial. *NPR*. July 3, 2024. https://www.npr.org/sections/goats-and-soda/2024/07/03/g-s1-7988/hiv-prevention-drug-clinical-trial (accessed 2024-07-23).
(10) *Gilead's Twice-Yearly Lenacapavir Demonstrated 100% Efficacy and Superiority to Daily Truvada® for HIV Prevention*. https://www.gilead.com/news-and-press/press-room/press-releases/2024/6/gileads-twiceyearly-lenacapavir-demonstrated-100-efficacy-and-superiority-to-daily-truvada-for-hiv-prevention (accessed 2024-07-23).
(11) *Gilead to Highlight Landmark Progress in Research Across HIV Prevention, Treatment and Cure Programs at AIDS 2024*. https://www.gilead.com/news-and-press/press-room/press-releases/2024/7/gilead-to-highlight-landmark-progress-in-research-across-hiv-prevention-treatment-and-cure-programs-at-aids-2024 (accessed 2024-07-23).
(12) Allan, K. M.; Batten, A. L.; Brizgys, G.; Dhar, S.; Doxsee, I. J.; Goldberg, A.; Heumann, L. V.; Huang, Z.; Kadunce, N. T.; Kazerani, S.; Lew, W.; Ngo, V. X.; O'keefe, B. M.; Rainey, T. J.; Roberts, B. J.; Shi, B.; Steinhuebel, D. P.; Tse, W. C.; Wagner, A. M.; Wang, X.; Wolckenhauer, S. A.; Wong, C. Y.; Zhang, J. R. Methods and Intermediates for Preparing a Therapeutic Compound Useful in the Treatment of Retroviridae Viral Infection. WO2019161280A1, August 22, 2019.
(13) Bauer, L. E.; Gorman, E. M.; Mulato, A. S.; Rhee, M. S.; Rowe, C. W.; Sellers, S. P.; Stefanidis, D.; Tse, W. C.; Yant, S. R.; Chiu, A. Capsid Inhibitors for the Treatment of Hiv. WO2020018459A1, January 23, 2020. https://patents.google.com/patent/WO2020018459A1/en?oq=WO%C2%A02020018459 (accessed 2021-02-17).
(14) Graupe, M.; Henry, S. J.; Link, J. O.; Rowe, C. W.; Saito, R. D.; Schroeder, S. D.; Stefanidis, D.; Tse, W. C.; Zhang, J. R. Therapeutic Compounds Useful for the

Prophylactic or Therapeutic Treatment of an Hiv Virus Infection. WO2018035359A1, February 22, 2018.

(15) Du, Z.; Farand, J.; Guney, T.; Kato, D.; Link, J. O.; Mack, J. B. C.; Mun, D. M.; Watkins, W. J.; Zhang, J. R. Therapeutic Compounds for HIV Virus Infection. WO2023102529A1, June 8, 2023.

(16) Link, J. O.; Rhee, M. S.; Tse, W. C.; Zheng, J.; Somoza, J. R.; Rowe, W.; Begley, R.; Chiu, A.; Mulato, A.; Hansen, D.; Singer, E.; Tsai, L. K.; Bam, R. A.; Chou, C.-H.; Canales, E.; Brizgys, G.; Zhang, J. R.; Li, J.; Graupe, M.; Morganelli, P.; Liu, Q.; Wu, Q.; Halcomb, R. L.; Saito, R. D.; Schroeder, S. D.; Lazerwith, S. E.; Bondy, S.; Jin, D.; Hung, M.; Novikov, N.; Liu, X.; Villaseñor, A. G.; Cannizzaro, C. E.; Hu, E. Y.; Anderson, R. L.; Appleby, T. C.; Lu, B.; Mwangi, J.; Liclican, A.; Niedziela-Majka, A.; Papalia, G. A.; Wong, M. H.; Leavitt, S. A.; Xu, Y.; Koditek, D.; Stepan, G. J.; Yu, H.; Pagratis, N.; Clancy, S.; Ahmadyar, S.; Cai, T. Z.; Sellers, S.; Wolckenhauer, S. A.; Ling, J.; Callebaut, C.; Margot, N.; Ram, R. R.; Liu, Y.-P.; Hyland, R.; Sinclair, G. I.; Ruane, P. J.; Crofoot, G. E.; McDonald, C. K.; Brainard, D. M.; Lad, L.; Swaminathan, S.; Sundquist, W. I.; Sakowicz, R.; Chester, A. E.; Lee, W. E.; Daar, E. S.; Yant, S. R.; Cihlar, T. Clinical Targeting of HIV Capsid Protein with a Long-Acting Small Molecule. *Nature* **2020**, *584* (7822), 614–618. https://doi.org/10.1038/s41586-020-2443-1.

(17) Gillis, E. P.; Parcella, K.; Bowsher, M.; Cook, J. H.; Iwuagwu, C.; Naidu, B. N.; Patel, M.; Peese, K.; Huang, H.; Valera, L.; Wang, C.; Kieltyka, K.; Parker, D. D.; Simmermacher, J.; Arnoult, E.; Nolte, R. T.; Wang, L.; Bender, J. A.; Frennesson, D. B.; Saulnier, M.; Wang, A. X.; Meanwell, N. A.; Belema, M.; Hanumegowda, U.; Jenkins, S.; Krystal, M.; Kadow, J. F.; Cockett, M.; Fridell, R. Potent Long-Acting Inhibitors Targeting the HIV-1 Capsid Based on a Versatile Quinazolin-4-One Scaffold. *J. Med. Chem.* **2023**, *66* (3), 1941–1954. https://doi.org/10.1021/acs.jmedchem.2c01732.

(18) Ebner, C.; Carreira, E. M. Cyclopropanation Strategies in Recent Total Syntheses. *Chem. Rev.* **2017**, *117* (18), 11651–11679. https://doi.org/10.1021/acs.chemrev.6b00798.

(19) Jacobsen, E. N.; Zhang, W.; Muci, A. R.; Ecker, J. R.; Deng, L. Highly Enantioselective Epoxidation Catalysts Derived from 1,2-Diaminocyclohexane. *J. Am. Chem. Soc.* **1991**, *113* (18), 7063–7064. https://doi.org/10.1021/ja00018a068.

(20) Brandes, B. D.; Jacobsen, E. N. Highly Enantioselective, Catalytic Epoxidation of Trisubstituted Olefins. *J. Org. Chem.* **1994**, *59* (16), 4378–4380. https://doi.org/10.1021/jo00095a009.

(21) Alam, M.; Wise, C.; Baxter, C. A.; Cleator, E.; Walkinshaw, A. Development of a Robust Procedure for the Copper-Catalyzed Ring-Opening of Epoxides with Grignard Reagents. *Org. Process Res. Dev.* **2012**, *16* (3), 435–441. https://doi.org/10.1021/op200329x.

(22) Xiao, H.-X.; Yan, Q.-X.; He, Z.-H.; Zou, Z.-B.; Le, Q.-Q.; Chen, T.-T.; Cai, B.; Yang, X.-W.; Luo, S.-L. Total Synthesis and Anti-Inflammatory Bioactivity of (−)-Majusculoic Acid and Its Derivatives. *Mar. Drugs* **2021**, *19* (6), 288. https://doi.org/10.3390/md19060288.

(23) Raheem, I. T.; Breslin, M. J.; Bruno, J.; Cabalu, T. D.; Cooke, A.; Cox, C. D.; Cui, D.; Garson, S.; Gotter, A. L.; Fox, S. V.; Harrell, C. M.; Kuduk, S. D.; Lemaire, W.; Prueksaritanont, T.; Renger, J. J.; Stump, C.; Tannenbaum, P. L.; Williams, P. D.; Winrow, C. J.; Coleman, P. J. Discovery of Piperidine Ethers as Selective Orexin Receptor

Antagonists (SORAs) Inspired by Filorexant. *Bioorg. Med. Chem. Lett.* **2015**, *25* (3), 444–450. https://doi.org/10.1016/j.bmcl.2014.12.056.
(24) Hodgson, D.; Chung, Y.; Paris, J.-M. Intramolecular Cyclopropanation of Epichlorohydrin-Derived Unsaturated Chlorohydrins. *Synthesis* **2005**, *2005* (13), 2264–2266. https://doi.org/10.1055/s-2005-869973.
(25) Hodgson, D. M.; Chung, Y. K.; Paris, J.-M. Intramolecular Cyclopropanation of Unsaturated Terminal Epoxides. *J. Am. Chem. Soc.* **2004**, *126* (28), 8664–8665. https://doi.org/10.1021/ja047346k.
(26) Hodgson, D. M. C., Ying Kit; Paris, Jean-Marc. Intramolecular Cyclopropanation of Epichlorohydrin-Derived Unsaturated Chlorohydrins. *Synthesis* **2005**, *2005* (13), 2264–2266. https://doi.org/10.1055/s-2005-869973.
(27) Alorati, A. D.; Bio, M. M.; Brands, K. M. J.; Cleator, E.; Davies, A. J.; Wilson, R. D.; Wise, C. S. A Practical and Scaleable Synthesis of 1R,5S-Bicyclo[3.1.0]Hexan-2-One: The Development of a Catalytic Lithium 2,2,6,6-Tetramethylpiperidide (LTMP) Mediated Intramolecular Cyclopropanation of (R)-1,2-Epoxyhex-5-Ene. *Org. Process Res. Dev.* **2007**, *11* (3), 637–641. https://doi.org/10.1021/op700042w.
(28) Seyferth, D. The Grignard Reagents. *Organometallics* **2009**, *28* (6), 1598–1605. https://doi.org/10.1021/om900088z.
(29) Guthrie, D.; Saathoff, J. M.; Sahani, R. L.; Nunes De Souza, A.; Cook, D. W.; Hochstetler, S. R.; Burns, J. M.; Moazeni-Pourasil, R. S.; Wierzbicki, J.; Ahmad, S.; Laidlaw, G. M.; Gupton, B. F.; Shanahan, C. S.; Klumpp, D. A.; Jin, L. Synthetic Process Development of (R)-(+)-1,2-Epoxy-5-Hexene: An Important Chiral Building Block. *Org. Process Res. Dev.* **2024**. https://doi.org/10.1021/acs.oprd.4c00101.
(30) Anderson, N. G. *Practical Process Research & Development: A Guide for Organic Chemists*, Second edition.; Elsevier: Academic press, 2012.
(31) We found that the solution of **C5.3** with a higher content of water (e.g. KF > 0.5%) consumes more equivalents of n-BuLi to achieve a full conversion in the Hodgson reaction. A solution of **C5.3** with a KF < 0.3%, the Hodgson cyclopropanation proceeds smoothly with 1.1 eq n-BuLi.
(32) De Luca, L.; Giacomelli, G.; Porcheddu, A. A Very Mild and Chemoselective Oxidation of Alcohols to Carbonyl Compounds. *Org. Lett.* **2001**, *3* (19), 3041–3043. https://doi.org/10.1021/ol016501m.
(33) Liang, Y.-F.; Wu, K.; Song, S.; Li, X.; Huang, X.; Jiao, N. I2- or NBS-Catalyzed Highly Efficient α-Hydroxylation of Ketones with Dimethyl Sulfoxide. *Org. Lett.* **2015**, *17* (4), 876–879. https://doi.org/10.1021/ol5037387.
(34) Chen, C. F., Xinghua; Zhang, Guozhen; Zhao, Qin; Huang, Guosheng. An Efficient Method for the Synthesis of α-Hydroxyalkyl Aryl Ketones. *Synthesis* **2008**, *2008* (20), 3205–3208. https://doi.org/10.1055/s-0028-1083149.
(35) Zacuto, M. J.; Cai, D. α-Hydroxylation of Carbonyls Using Iodine. *Tetrahedron Lett.* **2005**, *46* (3), 447–450. https://doi.org/10.1016/j.tetlet.2004.11.092.
(36) Mancuso, A. J.; Huang, S.-L.; Swern, D. Oxidation of Long-Chain and Related Alcohols to Carbonyls by Dimethyl Sulfoxide "Activated" by Oxalyl Chloride. *J. Org. Chem.* **1978**, *43* (12), 2480–2482. https://doi.org/10.1021/jo00406a041.

(37) Kawaguchi, T.; Miyata, H.; Ataka, K.; Mae, K.; Yoshida, J. Room-Temperature Swern Oxidations by Using a Microscale Flow System. *Angew. Chem. Int. Ed.* **2005**, *44* (16), 2413–2416. https://doi.org/10.1002/anie.200462466.
(38) Dess, D. B.; Martin, J. C. Readily Accessible 12-I-5 Oxidant for the Conversion of Primary and Secondary Alcohols to Aldehydes and Ketones. *J. Org. Chem.* **1983**, *48* (22), 4155–4156. https://doi.org/10.1021/jo00170a070.
(39) Ley, S. V.; Norman, J.; Griffith, W. P.; Marsden, S. P. Tetrapropylammonium Perruthenate, Pr4N+RuO4-, TPAP: A Catalytic Oxidant for Organic Synthesis. *Synthesis* **1994**, *7*, 639–666. https://doi.org/10.1055/s-1994-25538.
(40) Albright, J. Donald.; Goldman, Leon. Dimethyl Sulfoxide-Acid Anhydride Mixtures for the Oxidation of Alcohols. *J. Am. Chem. Soc.* **1967**, *89* (10), 2416–2423. https://doi.org/10.1021/ja00986a031.
(41) Bur, S. K.; Padwa, A. The Pummerer Reaction: Methodology and Strategy for the Synthesis of Heterocyclic Compounds. *Chem. Rev.* **2004**, *104* (5), 2401–2432. https://doi.org/10.1021/cr020090l.
(42) Reyes-Rodríguez, G. J.; Algera, R. F.; Collum, D. B. Lithium Hexamethyldisilazide-Mediated Enolization of Acylated Oxazolidinones: Solvent, Cosolvent, and Isotope Effects on Competing Monomer- and Dimer-Based Pathways. *J. Am. Chem. Soc.* **2017**, *139* (3), 1233–1244. https://doi.org/10.1021/jacs.6b11354.
(43) Knorr, L. Synthese von Pyrrolderivaten. *Berichte Dtsch. Chem. Ges.* **1884**, *17* (2), 1635–1642. https://doi.org/10.1002/cber.18840170220.
(44) Yadav, C. H.; Medarametla, V. 1,1,1,-TRIFLUORO METHYL KETONE AND ITS REACTION WITH GRIGNARD REAGENT. **2023**, No. 5.
(45) Lal, G. S.; Pez, G. P.; Pesaresi, R. J.; Prozonic, F. M. Bis(2-Methoxyethyl)Aminosulfur Trifluoride: A New Broad-Spectrum Deoxofluorinating Agent with Enhanced Thermal Stability. *Chem. Commun.* **1999**, No. 2, 215–216. https://doi.org/10.1039/A808517J.
(46) Beaulieu, F.; Beauregard, L.-P.; Courchesne, G.; Couturier, M.; LaFlamme, F.; L'Heureux, A. Aminodifluorosulfinium Tetrafluoroborate Salts as Stable and Crystalline Deoxofluorinating Reagents. *Org. Lett.* **2009**, *11* (21), 5050–5053. https://doi.org/10.1021/ol902039q.
(47) Melvin, P. R.; Ferguson, D. M.; Schimler, S. D.; Bland, D. C.; Sanford, M. S. Room Temperature Deoxyfluorination of Benzaldehydes and α-Ketoesters with Sulfuryl Fluoride and Tetramethylammonium Fluoride. *Org. Lett.* **2019**, *21* (5), 1350–1353. https://doi.org/10.1021/acs.orglett.9b00054.
(48) Hayashi, H.; Sonoda, H.; Fukumura, K.; Nagata, T. 2,2-Difluoro-1,3-Dimethylimidazolidine (DFI). A New Fluorinating Agent. *Chem. Commun.* **2002**, No. 15, 1618–1619. https://doi.org/10.1039/B204471D.
(49) Lal, G. S.; Lobach, E.; Evans, A. Fluorination of Thiocarbonyl Compounds with Bis(2-Methoxyethyl)Aminosulfur Trifluoride (Deoxo-Fluor Reagent): A Facile Synthesis of Gem-Difluorides. *J. Org. Chem.* **2000**, *65* (16), 4830–4832. https://doi.org/10.1021/jo000020j.
(50) Umemoto, T.; Singh, R. P.; Xu, Y.; Saito, N. Discovery of 4-Tert-Butyl-2,6-Dimethylphenylsulfur Trifluoride as a Deoxofluorinating Agent with High Thermal

Stability as Well as Unusual Resistance to Aqueous Hydrolysis, and Its Diverse Fluorination Capabilities Including Deoxofluoro-Arylsulfinylation with High Stereoselectivity. *J. Am. Chem. Soc.* **2010**, *132* (51), 18199–18205. https://doi.org/10.1021/ja106343h.

(51) L'Heureux, A.; Beaulieu, F.; Bennett, C.; Bill, D. R.; Clayton, S.; LaFlamme, F.; Mirmehrabi, M.; Tadayon, S.; Tovell, D.; Couturier, M. Aminodifluorosulfinium Salts: Selective Fluorination Reagents with Enhanced Thermal Stability and Ease of Handling,. *J. Org. Chem.* **2010**, *75* (10), 3401–3411. https://doi.org/10.1021/jo100504x.

(52) Fujimoto, T.; Ritter, T. PhenoFluorMix: Practical Chemoselective Deoxyfluorination of Phenols. *Org. Lett.* **2015**, *17* (3), 544–547. https://doi.org/10.1021/ol5035518.

(53) Turkman, N.; An, L.; Pomerantz, M. One-Pot Desulfurative−Fluorination−Bromination. Synthesis of 2,5-Dibromo-3-(1,1-Difluoroalkyl)Thiophenes. *Org. Lett.* **2010**, *12* (19), 4428–4430. https://doi.org/10.1021/ol101907k.

(54) Ivasyshyn, V.; Smit, H.; Chiechi, R. C. Synthesis of a Hominal Bis(Difluoromethyl) Fragment. *ACS Omega* **2019**, *4* (9), 14140–14150. https://doi.org/10.1021/acsomega.9b02131.

(55) Berglund, R. A.; Fuchs, P. L. Synthesis of Fluorinated Dienylic Stannanes Via the Wadsworth-Emmons Reaction. *Synth. Commun.* **1989**, *19* (11–12), 1965–1980. https://doi.org/10.1080/00397918908052589.

(56) Nicolaou, K. C.; Dolle, R. E.; Papahatjis, D. P. Practical Synthesis of Oligosaccharides. Partial Synthesis of Avermectin B1a. *J. Am. Chem. Soc.* **1984**, *106* (15), 4189–4192. https://doi.org/10.1021/ja00327a021.

(57) Sondej, S. C.; Katzenellenbogen, J. A. Gem-Difluoro Compounds: A Convenient Preparation from Ketones and Aldehydes by Halogen Fluoride Treatment of 1,3-Dithiolanes. *J. Org. Chem.* **1986**, *51* (18), 3508–3513. https://doi.org/10.1021/jo00368a022.

(58) Welch, F. J. Polymerization of Styrene by N-Butyllithium. II. Effect of Lewis Acids and Bases1. *J. Am. Chem. Soc.* **1960**, *82* (23), 6000–6005. https://doi.org/10.1021/ja01508a009.

(59) Emma, M. G.; Tamburrini, A.; Martinelli, A.; Lombardo, M.; Quintavalla, A.; Trombini, C. A Simple and Efficient Protocol for Proline-Catalysed Asymmetric Aldol Reaction. *Catalysts* **2020**, *10* (6), 649. https://doi.org/10.3390/catal10060649.

(60) Trost, B. M.; Brindle, C. S. The Direct Catalytic Asymmetric Aldol Reaction. *Chem. Soc. Rev.* **2010**, *39* (5), 1600. https://doi.org/10.1039/b923537j.

(61) Luo, J.; Tan, R.; Kong, Y.; Li, C.; Yin, D. Effect of Additives on L-Proline Catalyzed Direct Asymmetric Aldol Reactions. *Chin. J. Catal.* **2012**, *33* (7–8), 1133–1138. https://doi.org/10.1016/S1872-2067(11)60394-X.

(62) List, B.; Lerner, R. A.; Barbas, C. F. Proline-Catalyzed Direct Asymmetric Aldol Reactions. *J. Am. Chem. Soc.* **2000**, *122* (10), 2395–2396. https://doi.org/10.1021/ja994280y.

(63) Sakthivel, K.; Notz, W.; Bui, T.; Barbas, C. F. Amino Acid Catalyzed Direct Asymmetric Aldol Reactions: A Bioorganic Approach to Catalytic Asymmetric Carbon−Carbon Bond-Forming Reactions. *J. Am. Chem. Soc.* **2001**, *123* (22), 5260–5267. https://doi.org/10.1021/ja010037z.

(64) Bahmanyar, S.; Houk, K. N.; Martin, H. J.; List, B. Quantum Mechanical Predictions of the Stereoselectivities of Proline-Catalyzed Asymmetric Intermolecular Aldol Reactions. *J. Am. Chem. Soc.* **2003**, *125* (9), 2475–2479. https://doi.org/10.1021/ja028812d.
(65) Funabiki, K.; Yamamoto, H.; Nagaya, H.; Matsui, M. Proline-Catalyzed Direct Asymmetric Aldol Reaction of Trifluoroacetaldehyde Ethyl Hemiacetal with Ketones. *Tetrahedron Lett.* **2006**, *47* (31), 5507–5510. https://doi.org/10.1016/j.tetlet.2006.05.165.
(66) Ishii, A.; Kojima, J.; Mikami, K. Asymmetric Catalytic Friedel−Crafts Reaction of Silyl Enol Ethers with Fluoral: A Possible Mechanism of the Mukaiyama-Aldol Reactions. *Org. Lett.* **1999**, *1* (12), 2013–2016. https://doi.org/10.1021/ol990330s.
(67) Sarabèr, F. C. E.; Dratch, S.; Bosselaar, G.; Jansen, B. J. M.; de Groot, A. Domino Mukaiyama–Michael Reactions in the Synthesis of Polycyclic Systems. *Tetrahedron* **2006**, *62* (8), 1717–1725. https://doi.org/10.1016/j.tet.2005.11.059.
(68) Claraz, A.; Oudeyer, S.; Levacher, V. Enantioselective Desymmetrization of Prochiral Ketones via an Organocatalytic Deprotonation Process. *Tetrahedron Asymmetry* **2013**, *24* (12), 764–768. https://doi.org/10.1016/j.tetasy.2013.05.011.
(69) Kubota, T.; Iijima, M.; Tanaka, T. Facile Synthesis of α-Trifluoromethylated Alcohols from Trifluoroacetaldehyde Ethyl Hemiacetal. *Tetrahedron Lett.* **1992**, *33* (10), 1351–1354. https://doi.org/10.1016/S0040-4039(00)91620-4.
(70) Srivastava, N.; Ha, H.-J. Highly Efficient and Stereoselective Mukaiyama Aldol Reaction with Chiral Aziridine-2-Carboxaldehyde and Its Synthetic Applications. *Asian J. Org. Chem.* **2022**, *11* (1), e202100567. https://doi.org/10.1002/ajoc.202100567.
(71) Zhou, Y.; Yang, D.; Luo, G.; Zhao, Y.; Luo, Y.; Xue, N.; Qu, J. Highly Selective Trifluoroacetic Ester/Ketone Metathesis: An Efficient Approach to Trifluoromethyl Ketones and Esters. *Tetrahedron* **2014**, *70* (31), 4668–4674. https://doi.org/10.1016/j.tet.2014.05.017.
(72) Kitanosono, T.; Kobayashi, S. Mukaiyama Aldol Reactions in Aqueous Media. *Adv. Synth. Catal.* **2013**, *355* (16), 3095–3118. https://doi.org/10.1002/adsc.201300798.
(73) Kan, S. B. J.; Ng, K. K.-H.; Paterson, I. The Impact of the Mukaiyama Aldol Reaction in Total Synthesis. *Angew. Chem. Int. Ed.* **2013**, *52* (35), 9097–9108. https://doi.org/10.1002/anie.201303914.
(74) Matsuo, J.; Murakami, M. The Mukaiyama Aldol Reaction: 40 Years of Continuous Development. *Angew. Chem. Int. Ed.* **2013**, *52* (35), 9109–9118. https://doi.org/10.1002/anie.201303192.